Genetics Analysis of Standing Variation for Floral Morphology and Fitness Components in a Natural Population of *Mimulus guttatus* (common monkeyflower)

by

Young Wha Lee

University Program in Genetics and Genomics
Duke University

Date:_____
Approved:

_____
John H. Willis, Supervisor

_____
Mark Rausher, Chair

_____
John K. Kelly

_____
Tom Mitchell-Olds

_____
Mohamed A.F. Noor

Dissertation submitted in partial fulfillment of
the requirements for the degree of Doctor of Philosophy in the
University Program in Genetics and Genomics
in the Graduate School of Duke University

2009

ABSTRACT

Genetics Analysis of Standing Variation for Floral Morphology and Fitness Components

in a Natural Population of *Mimulus guttatus* (common monkeyflower)

by

Young Wha Lee

University Program in Genetics and Genomics
Duke University

Date:_____
Approved:

_____
John H. Willis, Supervisor

_____
Mark Rausher, Chair

_____
John K. Kelly

_____
Tom Mitchell-Olds

_____
Mohamed A.F. Noor

An abstract of a dissertation submitted in partial fulfillment of
the requirements for the degree of Doctor of Philosophy in the
University Program in Genetics and Genomics
in the Graduate School of Duke University

2009

Copyright by
Young Wha Lee
2009

Abstract

An unresolved problem in evolutionary biology is the nature of forces that maintain standing variation for quantitative traits. In this study we take advantage of newly developed genomic resources to understand how variation is maintained for flower size and fitness components in a natural population of annual *Mimulus guttatus* in the Oregon Cascades. Extensive inbreeding depression has been documented in this population for fertility and viability (Willis 1999 a,b), while previous biometric experiments have demonstrated that some of the floral variation in this site is due to common alleles perhaps maintained by balancing selection (Kelly and Willis 2001, Kelly 2003). Detailed comparison of the genetic architecture of these two categories of traits can clarify the relative contributions of mutation versus selection in maintaining trait variation within populations as well as the relevance of standing variation for trait diversification.

We present here the results from a large scale effort to dissect variation for flower size and a suite of genetically correlated traits. In 3 independent F2 mapping populations we mapped QTLs for floral morphology (flower width and length, pistil length, and stamen length), flowering time, and leaf size. We also mapped segregation distortion loci and QTLs for fertility components (pollen viability and seed set) that exhibit inbreeding depression. We compare the genetic architecture of these two sets of

traits and find clear differences. Morphological traits and flowering time are polygenic and QTLs are generally additive. In contrast, deleterious QTLs associated with segregation distortion or fertility are partially recessive and include major QTLs. There is also little co-localization between morphological/flowering time and fertility QTLs. The analysis suggests that the genetic basis of segregating variation in morphology is fundamentally different from traits exhibiting inbreeding depression. Further, there is considerable variation in the extant of pleiotropy exhibited by QTLs for morphological traits as well as flowering time and we report that epistasis contributes to the standing variation for these traits. The analysis suggests that the standing variation is relevant for trait diversification and that the variation in floral allometry, plant form, and life history observed in the *guttatus* species complex could have readily evolved from the standing variation.

Dedication

To my parents.

Contents

Abstract iv

List of Tables xi

List of Figures xiii

Acknowledgements xvii

1. The genetic architecture of inbreeding depression in a mostly outcrossing population of common monkeyflower (*Mimulus guttatus*) 1

1.1 Introduction 1

1.2 Materials and Methods 5

1.2.1 Study system 5

1.2.2 Generation of three F2 mapping populations 5

1.2.3 Tissue collection, DNA extraction, and marker genotyping 7

1.2.4 Phenotyping pollen viability, pollen number, and seedset 8

1.2.6 Linkage map construction 8

1.2.7 Transmission Ratio Distortion Loci (TRDL) mapping 9

1.2.8 Quantitative Trait Loci (QTL) mapping 10

1.2.9 Inferring mode of action for TRDLs 13

1.3 Results 13

1.3.1 Three independent F2 linkage maps of the Iron Mountain monkeyflower population 13

1.3.2 Gene based markers reveal a segregating chromosomal inversion unique to Iron Mountain 20

1.3.3 All three mapping populations are polymorphic for a verified meiotic drive locus on LG11 23

1.3.4 Transmission Ratio Distortion Loci (TRDLs) 24

1.3.5 Mode of gene action for verified TRDLs 30

1.3.6 Multi-dimensional epistasis contributes to transmission ratio distortion 35

1.3.7 Quantitative Trait Loci (QTLs) for male and female fertility 37

1.3.8 Mode of action for male and female fertility QTLs 42

1.3.9 Additive-dominant epistasis contributes to standing variation for male and female fertility 45

1.3.10 Environment dependent epistasis for pollen viability between meiotic drive and inversion alleles 47

1.4 Discussion 48

1.4.1 Linkage map construction and identification of TRDL in the guttatus species complex 48

1.4.2 Mapping suggests that both mutation selection balance and balancing selection contributes to the maintenance of fitness variation 50

1.4.3 Implications of epistasis for relevance of standing variation for adaptation 52

1.4.4 Implications of epistasis and environmental dependence for the evolution of selfing 53

1.4.5 Implications of epistasis for the dominance and overdominance hypotheses 54

1.4.6 Conclusions 54

2. Standing variation for floral morphology, leaf size, and time to flowering in a natural population of common monkeyflower *(Mimulus guttatus)* 55

2.1 Introduction 55

2.2 Materials and Methods 59

2.2.1 The study system: a variable population in a heterogeneous and extreme environment 59

2.2.2 Phenotypic measurements on morphological traits 61

2.2.3 Quantitative Trait Locus (QTL) mapping 61

2.2.4 Comparison with divergent QTLs 61

2.3 Results 62

2.3.1 Quantitative Trait Loci (QTLs) for standing variation in floral morphology, leaf size, and flowering time on Iron Mountain 62

2.3.1.1 Artificial selection for corolla width was effective. 68

2.3.1.2 Genetic basis of the correlated response to selection for corolla width 68

2.3.1.3 Individual traits in putatively pleiotropic loci affect the trait in the same direction 69

2.3.1.4 Consistency in individual dominance effects in pleiotropic QTLs for morphology. 69

2.3.1.5 Variation in individual dominance effects in pleiotropic QTLs for flowering time. 70

2.3.1.6 Many degrees of freedom in the standing variation for phenotypically correlated traits 70

2.3.1.7 Most flower size QTLs are unique to cross. 72

2.3.2 QTLs for corolla width do not co-localize with inbreeding depression QTLs . 74

2.3.3 Mode of action of QTLs for floral morphology, flowering time, and leaf width 76

2.3.4 Epistasis contributes to standing variation for morphological traits 79

2.3.5 Comparison with divergent QTLs 81

2.4 Discussion 83

2.4.1 Single biparental crosses are insufficient for describing the genetic architecture of standing variation. 83

2.4.2 Maintenance of standing variation for flower size on in the Iron Mountain population 84

2.4.3 Relevance of standing variation for adaptation 86

2.4.4 Many degrees of freedom for multivariate trait evolution 87

2.4.5 Epistasis and the evolution of the genetic variance and covariance 88

2.4.6 Conclusion 89

Bibliography 90

Biography 100

List of Tables

Table 1:Descriptive statistics for three linkage maps representing the Iron Mountain population. 14

Table 2: Summary of TRDL positions, parental origin, and associated genotype frequencies 30

Table 3: Mode of gene action for verified TRDLs. 32

Table 4: Epistatic TRDL pairs in the c4 population. P-values in bold survive Bonferroni correction at α=0.06. P-values <.05 that did not survive Bonferroni correction are also presented. * indicates epistatic TRDLs that had not met acceptance criteria in the original multipoint Bayesian mapping analysis. 36

Table 5: Mode of gene action for epistatic TRDLs of minor effect 37

Table 6: Summary of male and female fertility trait means and distributions. Pollen viability is % viable pollen, total pollen and supplemented seedset are counts per flower. Trait means are presented with phenotypic standard deviations. 37

Table 7:Summary of QTLs for male and female fertility. pv=pollen viability, pollen=total number of pollen per flower, seed=supplemented seed set. Each QTL is identified by cross, linkage group, and nearest marker. Additive effects are presented with d/|a| in parentheses, both in units of F2 phenotypic standard deviations. QTLs in boxes (both dotted and bold) were mapped in more than one cross. The QTL in bold type – c3:LG2:e274 – is a major deleterious QTL for all three measured components of fertility as well as viability 39

Table 8: Phenotypic means and distributions of F2 of ecologically relevant traits in the F2 mapping populations. All measures are in 100th inch, except for anthesis which is in days since seeding. Phenotypic standard deviations are presented in parentheses. cw=corolla width, cl= corolla length. 62

Table 9: Summary of QTLs for floral components, leaf width, and flowering time. The QTLs are organized by cross, and then by trait. For each QTL the additive effect *a* is reported with the additive-dominance ratio *d*/|*a*| in parentheses. Positive estimates of a indicate that the high parent carried the increasing allele, negative values indicate that the high parent carried the decreasing allele. Interpretation of d/|a| is as follows: d/|a|<-1 underdominant i.e. hets have smaller trait values than the homozygotes, -1 ≤

d/|a| <0 dominant for the decreasing allele (recessive for increasing allele), d/|a| = 0 additive, 0 < d/|a| ≤ 1 dominant for the increasing allele (recessive for decreasing allele), 1 < d/|a| overdominant i.e. hets have larger trait values than homozygotes. All units are in F2 phenotypic standard deviations. Pos=linkage map position in cM, marker=closest genotyped marker, cw=corolla width, cl=corolla length, ft=flowering time. Dotted boxes indicate shared corolla width QTL. Red boxes indicate variation in dominance in putatively pleiotropic loci. 64

List of Figures

Figure 1: Corolla width of Iron Mountain *Mimulus guttatus* in the high and low populations after 6 generations of selection. Representative individuals from the high and low population extremes are shown at left. Selection intensity 20% in both directions, for 6 generations of selection, n=1000 each generation each direction, outbred each generation to avoid purging. Figure courtesy of John K. Kelly. 6

Figure 2:Three selfed F2 linkage maps of the Iron Mountain *M. guttatus* population. The three maps are shown aligned together by linkage group. From left to right: mapping population c2, c3, and c4. Marker names in black are unique to a single cross. Marker names in red are shared across at least two of the three mapping populations. Black lines connect shared markers in adjacent linkage groups (i.e. shared markers between c2 and c3, and shared markers between c3 and c4). 18

Figure 3: A polymorphic inversion in Iron Mountain. A. Comparison of LG6 marker ordering in three different mapping populations. SFIM: *M. nasutus* x annual *M guttatus*, courtesy of Carrie Wu. 179x767: two randomly extracted Iron Mountain inbred lines. c3: from Figure 1. B. Identification of the putative inversion haplotype by phasing parental origin of shared F1 markers. Colors indicate allele identity, e.g. L2, H3, and L3 were homozygous for all markers, L2 and H3 for the same alleles. The putative inversion haplotype alleles are indicated by red. 21

Figure 4: Transmission ratio distortion loci in 3 selfed intra-population F2 crosses. There are 14 panels, with each panel representing a linkage group, ordered from top to bottom as c2, c3, and c4. Tick marks on the x axis are marker locations in Morgans; red tick marks indicate markers shared across all three linkage maps and may be used to infer whether TRDLS mapped on the same linkage group in different crosses co-localize. P-values for chi-square tests of deviation from Mendelian expectation for each marker are indicated above its map location (*<.1, **<.05, ***<.01, ****<.001, *****<.0001, ******<.00001, ********<.000001). The y-axis are counts from the posterior distribution of TRDL locations, grouped into 1 cM intervals. Posterior frequency for TRDL detection is indicated for each linkage group. Blue bars indicate TRDLs accepted for further analysis. The two red bars indicate epistatic TRDLs (see section 1.3.6). 29

Figure 5: Relationship between effect size (s) and dominance (h) in TRDLs. Red dots indicate "additive" TRDLs, blue dots indicate the remainder. h and s are probably overestimated for the c4 LG11 TRDL (indicated by an arrow). Underdominant TRDLs were not plotted. 34

Figure 6: Mode of gene action for male and female fertility trait QTLs. The additive dominance ratio is plotted against the absolute additive effect (units in phenotypic SD). C3:LG2:e274, a major sterility locus that affected all three fertility traits, is indicated by arrows. The inversion and driver was not included in this analysis. Overdominant QTLs were also excluded. 43

Figure 7: PVE (percent phenotypic F2 variation explained) for pollen viability and seed set QTLs. Red diamonds indicate the inversion and the drive loci, blue bars indicate the major effect sterility locus c3:LG2:e274. Blue diamonds are the remaining pollen viability and seed set loci in Table 7 (excluding overdominant loci). 45

Figure 8: Additive-dominant epistasis contributes to variation in male and female fertility. The pollen viability epistatic pair was mapped in c3; both seed set epistatic qtls were mapped in c4. z-axis: 2-locus QTL genotype means (in units of phenotypic standard deviations) estimated from the posterior distribution. H and L indicate High parent and Low parent QTL alleles, respectively 46

Figure 9: Environment-dependent epistasis between the meiotic drive and inversion alleles. D : driver allele, I: inversion allele. Individuals coded as "I" are all heterozygous for the inversion except for one homozygote. N=181 individuals. Above, 2-way anova for pollen viability with the inversion and drive genotypes. Below, genotypic means. The DD/I class had only 5 individuals, but was significantly different from all other 2 locus genotypes in pollen viability. 48

Figure 10: Extreme conditions define the growing season for the Iron Mountain monkeyflower population. 59

Figure 11: Heterogeneity in environmental conditions on Iron Mountain in the 2007 growing season. Time is on the horizontal axis, space on the vertical axis. In mid June, the lower slope was in full flower while the upper slope is just beginning to bolt. The water supply defines the length of the growing season. By mid July, all plants in the lower slope are dead, but plants survive near the tree line in the upper slope. 60

Figure 12: Many degrees of freedom in the standing genetic variation for phenotypically correlated traits. A. c3 LG8, orange line = corolla width, red line =corolla length, black line = length width ratio. Length width ratio QTLs coincide with regions of the genome that affect single traits i.e. corolla width. B. c3 LG8, purple line = stamen length, blue line = pistil length, black line = stigma anther separation. SA separation coincides with regions of the genome that affect single traits i.e. pistil length. Independent control of floral organs implies considerable variation for floral allometry. C.orange line = corolla

width, green line = leaf width. We present all 14 linkage groups. Pleiotropic and independent QTLs are both observed, suggesting leaf and flower size can evolve coordinately or independently of each other. Y-axis in all figures: 2logBF, Bayes factor for the inclusion of a specific genomic region in the QTL model. 72

Figure 13: Expectations for heterozygosity in the F1s after 6 generations of selection given a QTL of effect size a=0.1. Expectations for a=0.1 (lower than the average of a=~0.25 for QTLs mapped in this experiment) are presented because the average effect of a QTL substitution estimated in a biallelic cross decreases in the context of a population (Valdor et al 2007). A. Probability of obtaining one heterozygote in the right direction (blue) and wrong direction (pink) after 6 generations of selection from different starting allele frequencies. B. Probability of having 0,1,2,3 heterozygous F1s in the right direction. Blue dots = 0 heterozygous F1s, pink dots = 1 heterozygous F1, green dots = 2 heterozygous F1s, and red dots = 3 heterozygous F1s.....74

Figure 14: QTls affecting corolla width, seed set, and pollen inviability. Pollen number was excluded as it appears to have little influence on inbreeding depression for male fertility. c2, c3, and c4 mapping population results are stacked from top to bottom and we present all 14 linkage groups. Black lines = seed set or pollen viability QTLs. Orange lines = corolla width QTLs. Aside from the inversion (LG6) there are only 3 instances of co-localization between an inbreeding depression QTL and a corolla width QTL (indicated by a red star). Y-axis: 2logBF, Bayes factor for the inclusion of a specific genomic region in the QTL model.....75

Figure 15: Mode of gene action for morphology and flowering time QTLs. Absolute additive effects on the x-axis, dominance ratio in the y axis. QTLs in circles map to the same putatively pleiotropic loci. C4:LG10:e27 also effects pollen viability (see Figure 14). We also indicate the major sterility/viability locus c3:LG2:e274 (see section 1.3.7), which affects stamen length. 76

Figure 16: PVE (percent F2 variation explained) for morphology and flowering time QTLs. Two "major" QTLs, the same as highlighted within circles in Figure 15, account for most of the outlier loci (points within the circle, c4:LG4:e573 and c4:LG10:e27). The remaining outlier loci are all single trait QTL that affect pistil or stamen length (arrows). 78

Figure 17: Epistatic interactions affecting floral morphology. Four epistatic interactions are presented, described above by cross, trait(s) affected, and the type of interaction. a-d: additive by dominant, d-d: dominance by dominance, a-a: additive by additive. Z axis is trait values in phenotypic standard deviations. 80

Figure 18: QTLs for floral and leaf morphology divergence between the perennial and annual ecotypes of guttatus. All QTLs were in the right direction, i.e. the bigger perennial parent carried the increasing allele. 82

Acknowledgements

I would like to thank my advisors, John Willis and John Kelly, for their epic patience, for the trust they placed in me to carry things through, for their example as scholars and scientists, and their unstinting generosity as teachers.

(This is all true. Salute, profs.)

Thanks especially to John Willis for a thousand intangible day-to-day things: wisdom, *sanity* (and sometimes, insanity), general cheerleading, positive vibes of positive goodness, I don't know what all. In this place you created work gets done and people grow. I loved every minute.

All iterations of the Willis lab in my seven years at Duke were an awesome group of students. Thanks to my labmates past and present for the support network, whether in the form of manual labor, intellectual sounding board, the occasional pat on the back, the really occasional uplift out of the pit – and last but not least, for tolerating my hogging of thermal cyclers and greenhouse space!

Finally, thanks to my mother, dad, and little brother, for their love and support as I build a life in a land foreign to them in more ways than one.

1. The genetic architecture of inbreeding depression in a mostly outcrossing population of common monkeyflower (*Mimulus guttatus*)

1.1 Introduction

How is genetic variation maintained in natural populations? This is a question that has motivated evolutionary biologists in the last century, and it is still an unresolved question in the age of genomics (Barton and Keightley 2002, Mitchell-Olds et al 2008, Barton and Turelli 1989). The origin and maintenance of genetic variation was classically conceived as the deleterious mutation model versus the balance hypothesis (Lewontin 1974). Theoretical advances have since reframed the question as one of whether genetic variation is maintained by mutation selection balance in the face of stabilizing selection for a trait optimum versus various balancing selection hypotheses that incorporate pleiotropy and environmental heterogeneity. The theory is extensive (reviewed in Johnson and Barton 2005, Hedrick 2006) but models are still basically differentiated by whether mutation or selection determines the observed amount of heritable variation.

Closely related to the question of the maintenance of variation is the genetic basis of inbreeding depression and heterosis. Inbreeding depression is defined as the decrease in fitness observed in progeny with inbreeding. Heterosis is a term originating from applied genetics, and is the observation of hybrid vigor of F1 progeny over either inbred parent. Heterosis and inbreeding depression are thought to be converse aspects of the same phenomenon, i.e. the superiority in fitness of heterozygotes over

homozygote genotypes. Inbreeding depression is a general phenomenon in natural populations, widely observed across both the plant and animal kingdoms (Charlesworth and Charlesworth 1987, Crnocrak and Roff 1999, Husband and Schemske 1996), and appears to be a common feature of variation for fitness components.

There are three hypotheses pertaining to the genetic basis of inbreeding depression and heterosis: dominance, overdominance, and epistasis (Charlesworth and Charlesworth 1999.Hochholdinger and Hoecker 2007, Birchler et al 2003). In the dominance hypothesis, inbreeding depression is a result of the gene action of recessive deleterious alleles and heterosis results from complementation of such alleles with outcrossing. In the overdominance hypothesis, heterosis is caused by an inherent advantage in fitness in the heterozygote and inbreeding depression is caused by the loss of heterozygosity. Under this hypothesis alleles are maintained as polymorphisms by a form of balancing selection. Finally, epistasis explains differences in homozygote and heterozygote fitness as the result of complex interactions between alleles at two or more genes.

Much interest in inbreeding depression stems from its evolutionary consequences for the population's breeding system and for conservation genetics (Lande and Schemske 1985, Jarne and Charlesworth 1993, Tallmon et al 2004). Much interest also stems from its practical consequences for crop breeding in increasing yield (Springer and Stupar 2008). But, unraveling the causes of inbreeding depression may be also of much more general interest for the question of how standing variation originates.

This is because the genetic basis of inbreeding depression informs how variation is maintained within populations for traits such as fecundity and viability - traits closely related to fitness, for which there is a strong null expectation for the limiting role of mutation in controlling the observed amount of variation.

That is, the simplest, most straightforward explanation for inbreeding depression is that of deleterious mutations maintained by recurrent mutation, and this is consistent with the dominance hypothesis. The expectation that inbreeding depression is caused mainly by partially recessive deleterious alleles can be empirically tested by estimating the dominance coefficients of genetic variants causing inbreeding depression under a population genetic framework that that relates the change in fitness of traits (inbreeding load) with degree of inbreeding (reviewed in Charlesworth and Charlesworth 1987 and 1999, Lewontin 1974). But to date inconclusive results are often observed, as these approaches were limited to estimates of the deleterious effects of whole genomes or chromosomes, or population level correlations of heterozygosity and some fitness component.

QTL mapping methods can contribute to teasing out which of the three hypotheses apply by directly estimating the gene action of individual loci, although there are still problems with this approach (Carr and Dudash 2003). For example with linkage it is not possible distinguish between pseudo-overdominance and true overdominance without advanced generations of breeding. There are numerous mapping studies on heterosis and inbreeding depression for yield related traits in crop

species, with mixed evidence supporting all three hypotheses (Xiao et al 1995, Li et al 2001, Radoev et al 2008, Stuber et al 1992). There are only few examples of QTL mapping studies explicitly applied to the genetic basis of inbreeding depression in natural systems, but those few examples also support all three hypotheses. For example, Mitchell-Olds 1995 found evidence for overdominance in a putative viability locus exhibiting transmission ratio distortion, while a pine study (Remington and O'Malley 2000) concluded that embryonic viability loci detected as transmission ratio distortion in a linkage map were partially recessive. In addition, epistasis was found to contribute significantly to heterosis in Arabidopsis mapping studies explicitly designed to detect it (Melchinger et al 2007, Kusterer et al 2007).

Inbreeding depression in the Iron Mountain population of annual monkeyflowers has been extensively studied with somewhat conflicting results. Purging experiments and estimations of inbreeding load suggested that most inbreeding depression in this system is due to partially recessive, small effect deleterious alleles, in line with mutation selection balance and the dominance hypothesis (Willis 1999a, 1999b, 1999c). However, an explicit estimation of genetic variance components under the deleterious mutation model found that there was excess genetic variation for male fitness (a trait that was also assessed in Wilis 1999 a,b, and c) compared to the expectations of mutation selection balance (Kelly 2003). We further extend these studies on the causes of inbreeding depression on Iron Mountain by mapping QTLs that affect

male and female fertility as well as seed-to-flowering viability and estimating their gene action.

1.2 Materials and Methods

1.2.1 Study system

Mimulus guttatus (2n=28, Scrophulariacaea) is a self-compatible wildflower that grows throughout Western North America. It is the most common member of an eponymous species complex comprised of highly polytypic, partially interfertile subspecies (Vickery 1978) noted for their adaptive diversification as well as the independent evolution of multiple selfing lineages (Fenster and Ritland 1989, Ritland and Ritland 1994).

This study focuses on a population of monkeyflowers on Iron Mountain, a part of the Western Cascades of Oregon. The site is an alpine xeric meadow composed of a steep north facing slope at an elevation of 1470 m, over an area of ~600m^2. The population usually comprises tens of thousands of individuals each year, is bee-pollinated, and has a mixed mating system with an estimated selfing rate of 9-25% (Willis 1993, Sweigart 1999). The population shows no evidence of genetic structure (Sweigart et al 1999) or biparental inbreeding (Kelly and Willis 2002).

1.2.2 Generation of three F2 mapping populations

The parents in this experiment were extracted from the selection experiment detailed in Kelly 2008. Briefly, the starting materials are two phenotypically divergent

populations, created through six generations of bi-directional artificial selection on corolla width in a large experimental population derived from the wild population on Iron Mountain (1192 unrelated plants collected on 4 separate years). We assume that as crosses involved parents only 8 generations removed from the field, the segregation of variation in the crosses is reflective of variation present in the wild population. Recessive deleterious alleles causing inbreeding depression was expected to be carried intact through generations of selection in the greenhouse as the population was outbred at every generation and population size was large. We selected three "high parents" and three "low parents" from the extremes of the phenotypic distributions (Figure 1). Three independent F2 mapping populations, each of 384 individuals, were derived from selfing the F1s of crosses between a High and Low parent. The populations are by convention called c2, c3, and c4 mapping populations.

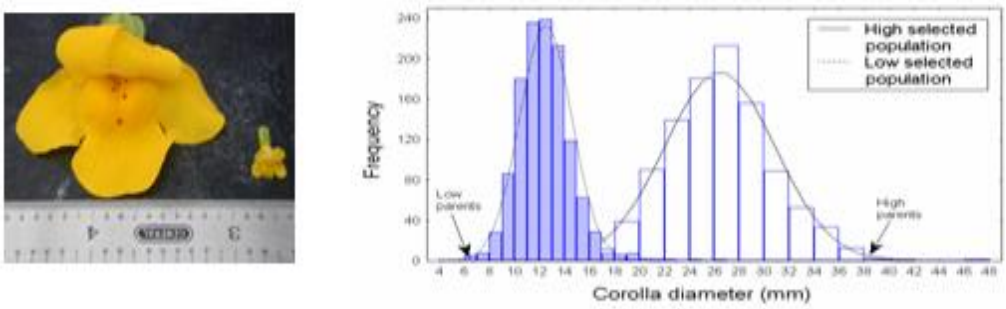

Figure 1: Corolla width of Iron Mountain *Mimulus guttatus* in the high and low populations after 6 generations of selection. Representative individuals from the high and low population extremes are shown at left. Selection intensity 20% in both directions, for 6 generations of selection, n=1000 each generation each direction, outbred each generation to avoid purging. Figure courtesy of John K. Kelly.

1.2.3 Tissue collection, DNA extraction, and marker genotyping

Bud meristem tissue was collected from each of 378, 384, and 384 F2 individuals of mapping population c2, c3, and c4c respectively and DNA extraction was done according to standard CTAB procedures (Kelly and Willis 1998). For wild collections whole plants were placed in dessicant and DNA was extracted with standard CTAB procedures after tissue was completely dried.

Almost all of the markers used for this study (prefixed with MgSTS – *M. g*uttatus *s*equence *t*agged *s*ite – or simply "e" – for expressed sequence tag) are exon-primed markers spanning introns. The forward primer was tagged in the 5′ end with fluorescent dye and the resulting labeled PCR products were run on ABI 3730 or 3700 Genetic Analyzers (Applied Biosystems, Fister City, CA). Genotypes were scored in Genemarker software (Softgenetics, State College, PA) based on the segregation of intron-length variable alleles. These markers are intended to be co-dominant and single copy, allowing genetics maps from different experiments to be tied together through markers in orthologous genes. Details for each MgSTS marker are publicly available on www.mimulusevolution.org.

To identify informative markers in each cross for map construction, the outbred parents and F1 individuals were screened for 748 MgSTS markers that had been successfully amplified in IM62, a standard inbred line derived from Iron Mountain (Sweigart et al 2004). PCR amplification in the F2s followed a standard touchdown

protocol (e.g. see Fishman and Willis 2005) with multiplexing and pooling based on expected allele sizes. Several microsatellite legacy markers (prefixed by "aat", Fishman and Willis 2002) and custom-designed markers (prefixed by "yw") were also amplified in each mapping population for the purpose of filling in large gaps of 30-plus cM.

1.2.4 Phenotyping pollen viability, pollen number, and seedset

Each F2 individual was phenotyped for pollen viability and pollen number on the first and second flower, as well as supplemented seedset on the third and fourth flower. The male fertility traits were measured following a protocol by Kelly et al 2003 which uses a Coulter Counter to sort pollen grains on the basis of size. This method takes advantage of a strong correlation between the size of the pollen grain and pollen viability as assessed by aniline blue staining. Supplemented seed set was done with a common pollen donor (IM62, a standard inbred line derived from Iron Mountain) for all flowers.

1.2.6 Linkage map construction

Missing or inaccurate genotypes can significantly affect map ordering (Hackett and Broadfoot 2003, Jansen et al 2001). Construction of the linkage maps was preceded by 3 iterative rounds of data quality control. We used JOINMAP 4.0 (Stam 1993) to construct preliminary maps by regression mapping and examined each marker for amount of missing data and for incidence of double crossovers. Markers with significant missing data (20% or more) were re-amplified depending on whether the marker was critical to fill a gap, otherwise it was discarded. Markers that had significant

numbers of double crossovers were either discarded, re-genotyped, had certain problematic individuals coded as "missing", was re-coded as dominant, or was re-amplified depending on the importance of the marker for map resolution. Special effort was made to identify and place markers that filled in large gaps and markers that were shared between crosses.

The final linkage map was created with the Kosambi mapping function using the maximum likelihood algorithm in JOINMAP 4.0, with standard defaults. We made two versions of linkage group 6 for each map as this chromosome exhibited extensive recombination suppression involving 20-30 markers in each map. One version was made using the maximum likelihood algorithm as above, with all but one representative marker in the suppressed recombination region deleted. Deleting excess markers in the region of suppressed recombination was necessary for mapping and permutation tests (see 1.2.8). It was also necessary because the maximum likelihood method is sensitive to double crossovers in densely genotyped regions and thus miscoding in the recombination suppressed region was interpreted as genetic distance. The second version of LG6 was made for the purpose of visualizing the recombination suppression. This version included all the genotyped markers on linkage group 6 and was created by regression mapping.

1.2.7 Transmission Ratio Distortion Loci (TRDL) mapping

Each marker was tested against Mendelian transmission expectations of 1:2:1 or 3:1 by chi-square tests in JOINMAP 4.0 (1d.f. for dominant and 2 d.f. for co-dominant

markers). The chi-square p-value for each marker was visualized in the framework of the linkage map in order to identify TRDLs, which are putatively due to viability selection (Luo et al 2005, Cheng et al 1996).

We further used the Bayesian multipoint mapping method devised by Vogl and Xu (2000) to detect and estimate the location of TRDLs. Claus Vogl very kindly provided an updated version of his program ANITA, which modified the method for backcrosses described in Vogl and Xu (2000) for a general cross with up to 4 alleles. Each linkage group was analyzed separately with 10000 iterations per linkage group. The maximum number of TRDL per group was set to 1, except for one case where it was set to 2 (mapping population c3, linkage group 2, where both linkage group ends were quite significantly distorted in opposite directions). Generally the chi-square p-values also suggested the presence of only one TRDL per linkage group. Experimentation showed that in several cases where chi-square tests suggested the presence of two TRDLs in a linkage group, but one TRDL was much more distorted than the other, ANITA was ineffective in detecting the second, smaller TRDL in addition to the larger distortion (the posterior distribution of locations concentrated on the bigger TRDL). .

1.2.8 Quantitative Trait Loci (QTL) mapping

Windows QTL Cartographer 2.5 (Wang et al 2007) was used for the initial mapping of QTLs by composite interval mapping (Zeng 1994). Model selection for background markers in QTL cartographer proceeded by forward backward selection with window sizes of 5 cM, 10 cM , and 15 cM and background marker numbers 15, 5, 10

for c3, c2, c4 respectively. We ran 1000 permutations per trait to get a genome wide 5% threshold (generally LR=14-17) and identified significant QTLs for each trait in each cross (results not presented). We also implemented multi-trait composite interval mapping (Jiang and Zeng 1995), but its utility was limited as the traits were not highly correlated. While some highly pleiotropic large effect QTLs were clearly identified, the polygenic nature of all traits and the labile correlational relationships among traits makes it difficult to 1) identify likelihood ratio peaks from the joint trait analysis (e.g. multiple jagged peaks across a linkage group without clear valleys between peaks), and 2) distinguish the individual contribution of single traits to the joint trait peaks along the chromosome (MCIM results are not presented).

The QTL cartographer CIM results were used to set the prior in Bayesian mapping as implemented in Rqtlbim (Yandell et al 2007, Yi et al 2007), and each trait was analyzed singly. In the Bayesian mapping framework, Markov chain Monte Carlo (MCMC) samples are drawn to estimate the posterior distribution of the genetic architecture of the trait (i.e. the number of loci, their locations, effects at each locus, epistatic interactions). The "best" model is estimated from the entire posterior sample by weighting each model with its posterior probability. The strength of evidence of inclusion of a particular QTL in the model can be seen by the Bayes factor for a locus, or the ratio of posterior to prior odds for the model with and without that QTL (by convention, 2logBF =2.1 is "high"). The estimated model is further refined in an anova

framework by stepwise backward elimination of QTLs, and only significant QTLs ($p<0.05$) were retained.

In our analysis, we made use of model selection tools in Rqtlbim to estimate the genetic architecture of each trait in each cross. First, we estimated the "best" pattern of the number and locations of QTLs and their interactions and assessed it as above. We also did explicit comparisons of the best model with reduced models where the QTL with the lowest p-value and/or any epistatic interactions were dropped. We further in some cases compared the best model with expanded models that included a smaller effect QTL (generally, 2logBF=2-3) that was not originally included in the best model. This was because 1) sometimes there was not a clear difference between the "best" model and a bigger model in terms of its posterior probability or Bayes factor or 2)in some cases a QTL that would have been accepted in CIM or MCIM was not included in the "best" model. We accepted the more conservative model in all comparisons. MCMC runs were assessed for convergence and in most cases standard defaults sufficed, except for 3 cases where we ran double the number of iterations.

QTLs were called as pleiotropic if the 50% highest posterior probability regions overlapped by containing one shared marker. This is simply observation and not a formal test for pleiotropy; multi-trait mapping is currently under development in Rqtlbim but not yet released (Banerjee et al 2008). Though the MCIM approach is problematic for our dataset we further compared our inference of pleiotropic QTLs from

the Bayesian mapping analysis with the peak locations of QTL identified in the MCIM analysis in QTL Cartographer (results not presented).

1.2.9 Inferring mode of action for TRDLs

A simple test for gametic selection was done by calculating w, or the gametic transmission frequency for the deleterious allele under a model of gametic selection (w=0.5 under neutrality), and testing against chi square expectations for genotype proportions. Under gametic selection the expected genotype proportions for AA, Aa, and aa are 0.5(1-w) : 0.5 : 0.5w, and w=(number of aa individuals)/(number of aa and AA individuals). We also calculated s, the selection coefficient, and h, the dominance coefficient assuming viability selection from the genotypic counts (expected genotype proportions 1 : 2(1-hs) : 1-s). The 95% confidence intervals for *h* assuming dominance or recessivity of the deleterious allele was generated by sampling 10000 times from the multinomial distribution for genotype proportions for a given *s* with *h* assumed to be 0 or 1. Finally, we conducted chi-square tests for non-independence of genotype proportions for every pair of mapped TRDLs, adjusted with Bonferroni correction for the number of tests.

1.3 Results

1.3.1 Three independent F2 linkage maps of the Iron Mountain monkeyflower population

The estimated linkage maps of mapping populations c2, c3, c4 are presented (Figure 2) with descriptive statistics (Table 1). All statistics were derived from the reduced version of the linkage maps where all but one marker in recombination

suppressed regions were deleted. Genotyping success rate for each population was 95.3%, 97.2 %, and 96.7% respectively.

Table 1:Descriptive statistics for three linkage maps representing the Iron Mountain population.

mapping population	N individuals	N markers	% co-dominant markers	% distorted markers (p<.01, .05)	total map length (cM)	genomewide average intermarker distance (cM)	estimated genome coverage (10,20 cM)
c2	373	172	87.2	6.4,15.7	1678.3	9	87.1%,98.3%
c3	383	175	93.7	12,20	1627.5	8.4	88.4%,98.6%
c4	382	165	89.7	19.4,29.7	1853.4	10.3	83.1%,97.2%

Most of the genotyped markers are co-dominant, enabling dominance estimation. Subsets of markers in all three mapping populations were significantly distorted in chi-square tests for Mendelian transmission, with the largest proportion in population c4. All three linkage maps resolved to the expected 14 linkage groups (2n=28), and were comparable in terms of map length and marker density. Taking the ends of linkage groups into account, total map length was calculated by adding 2s to the estimated length of each linkage group, where *s* equals the average intermarker distance for that linkage group. Assuming random distribution of markers, estimated genome coverage was calculated as $c=1-(e^{-2dn/L})$, the proportion of the genome within distance *d* of a marker, where *n* is the number of markers and *L* is total map length.

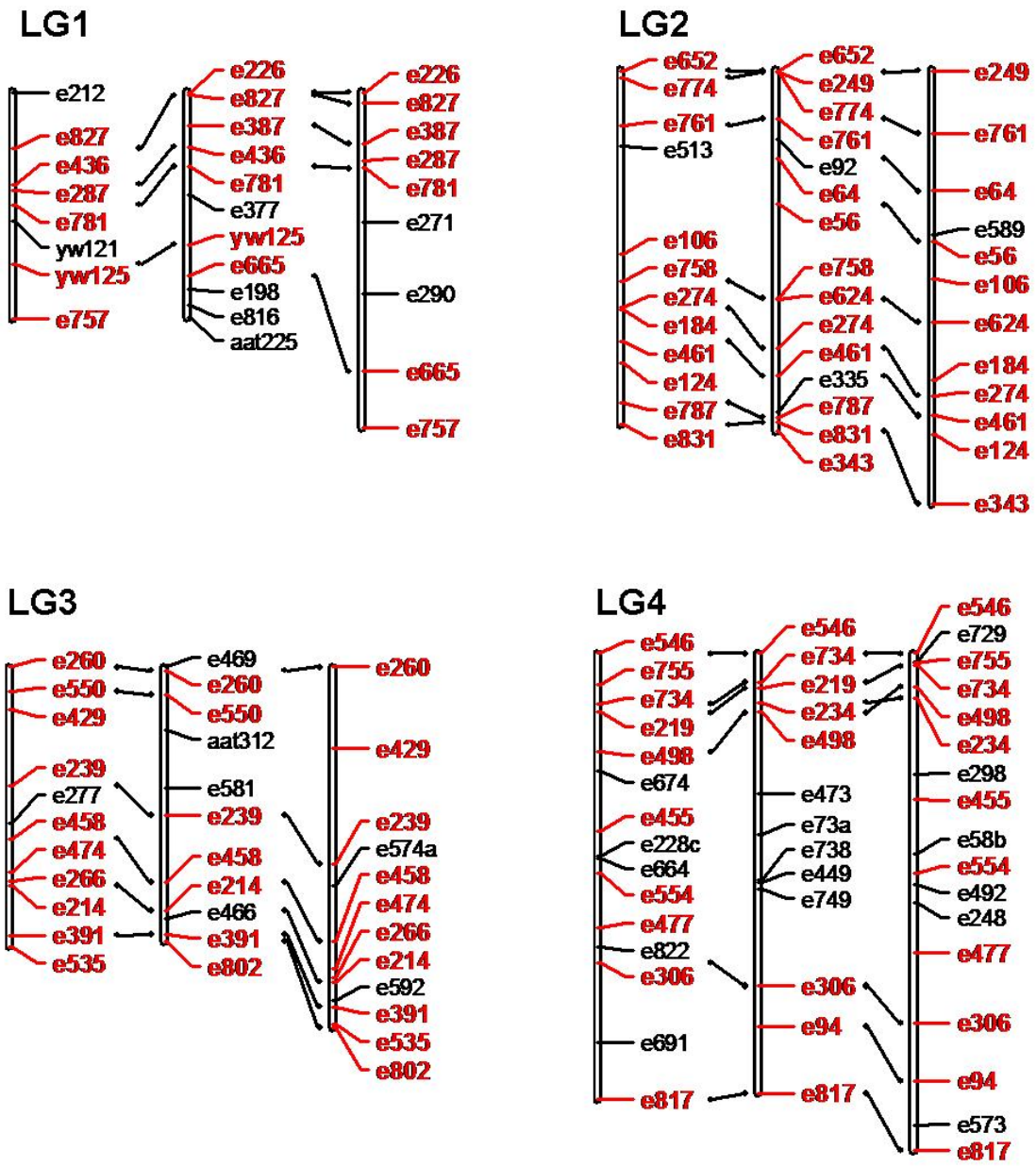
LG1
e212
e827
e436
e287
e781
yw121
yw125
e757
e226
e827
e387
e436
e781
e377
yw125
e665
e198
e816
aat225
e226
e827
e387
e287
e781
e271
e290
e665
e757
LG2
e652
e774
e761
e513
e106
e758
e274
e184
e461
e124
e787
e831
e652
e249
e774
e761
e92
e64
e56
e758
e624
e274
e461
e335
e787
e831
e343
e249
e761
e64
e589
e56
e106
e624
e184
e274
e461
e124
e343
LG3
e260
e550
e429
e239
e277
e458
e474
e266
e214
e391
e535
e469
e260
e550
aat312
e581
e239
e458
e214
e466
e391
e802
e260
e429
e239
e574a
e458
e474
e266
e214
e592
e391
e535
e802
LG4
e546
e755
e734
e219
e498
e674
e455
e228c
e664
e554
e477
e822
e306
e691
e817
e546
e734
e219
e234
e498
e473
e73a
e738
e449
e749
e306
e94
e817
e546
e729
e755
e734
e498
e234
e298
e455
e58b
e554
e492
e248
e477
e306
e94
e573
e817

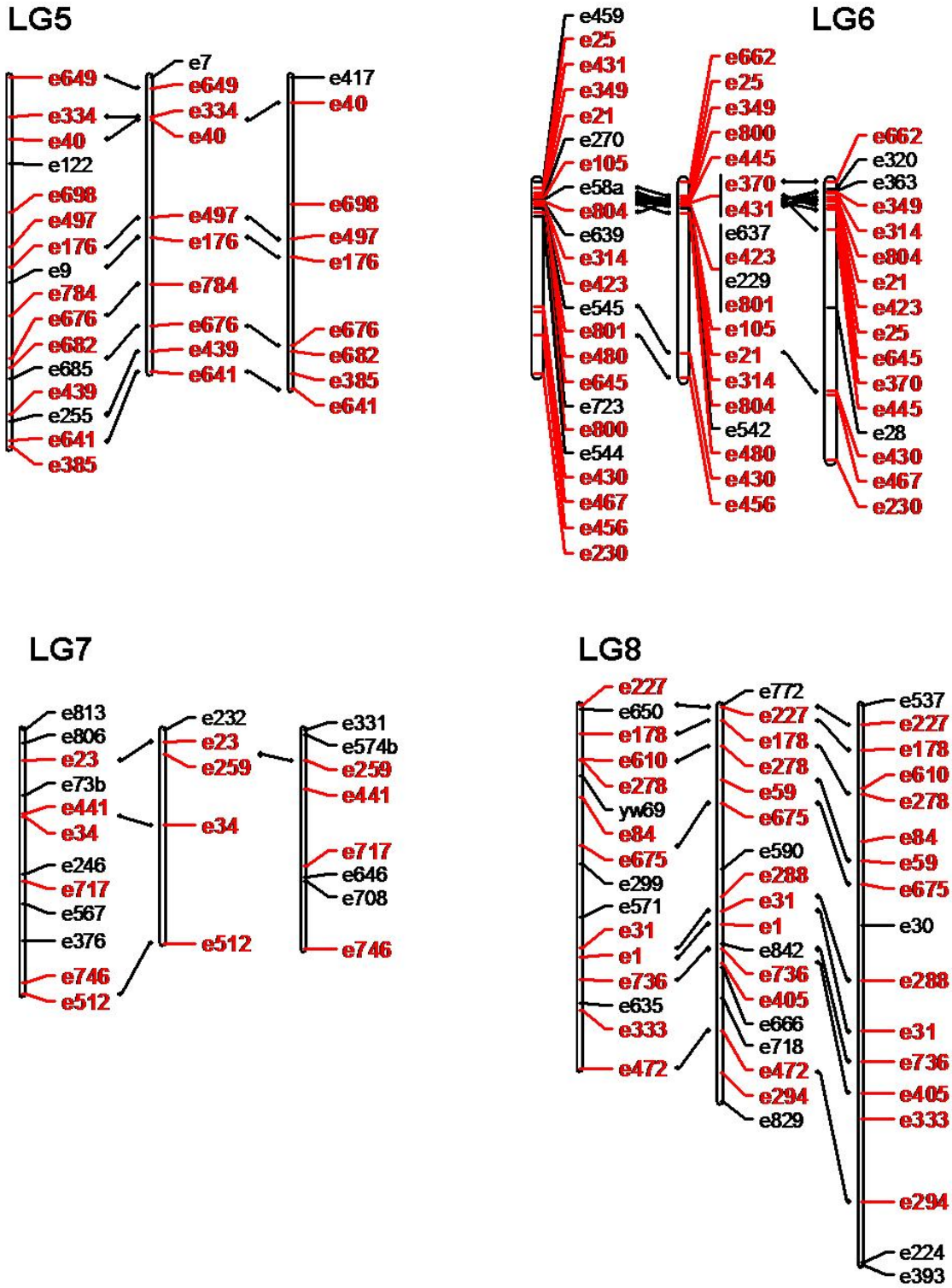
LG5
e649
e334
e40
e122
e698
e497
e176
e9
e784
e676
e682
e685
e439
e255
e641
e385
e7
e649
e334
e40
e497
e176
e784
e676
e439
e641
e417
e40
e698
e497
e176
e676
e682
e385
e641
LG6
e459
e25
e431
e349
e21
e270
e105
e58a
e804
e639
e314
e423
e545
e801
e480
e645
e723
e800
e544
e430
e467
e456
e230
e662
e25
e349
e800
e445
e370
e431
e637
e423
e229
e801
e105
e21
e314
e804
e542
e480
e430
e456
e662
e320
e363
e349
e314
e804
e21
e423
e25
e645
e370
e445
e28
e430
e467
e230
LG7
e813
e806
e23
e73b
e441
e34
e246
e717
e567
e376
e746
e512
e232
e23
e259
e34
e512
e331
e574b
e259
e441
e717
e646
e708
e746
LG8
e227
e650
e178
e610
e278
yw69
e84
e675
e299
e571
e31
e1
e736
e635
e333
e472
e772
e227
e178
e278
e59
e675
e590
e288
e31
e1
e842
e736
e405
e666
e718
e472
e294
e829
e537
e227
e178
e610
e278
e84
e59
e675
e30
e288
e31
e736
e405
e333
e294
e224
e393

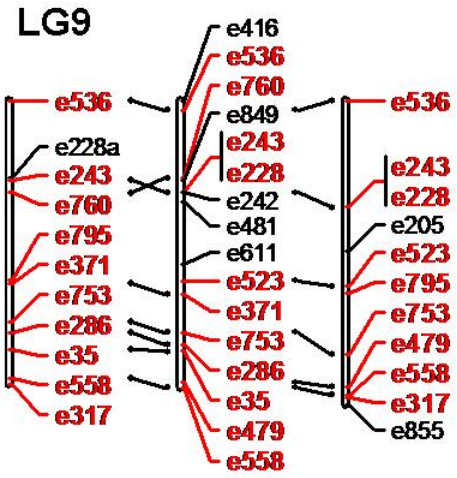
LG9
e536
e228a
e243
e760
e795
e371
e753
e286
e35
e558
e317
e416
e536
e760
e849
e243
e228
e242
e481
e611
e523
e371
e753
e286
e35
e479
e558
e536
e243
e228
e205
e523
e795
e753
e479
e558
e317
e855

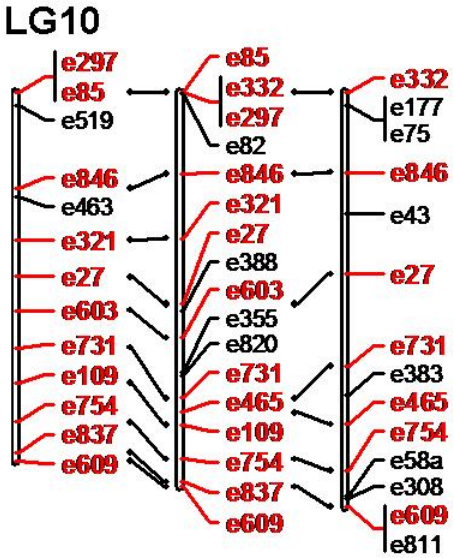
LG10
e297
e85
e519
e846
e463
e321
e27
e603
e731
e109
e754
e837
e609
e85
e332
e297
e82
e846
e321
e27
e388
e603
e355
e820
e731
e465
e109
e754
e837
e609
e332
e177
e75
e846
e43
e27
e731
e383
e465
e754
e58a
e308
e609
e811

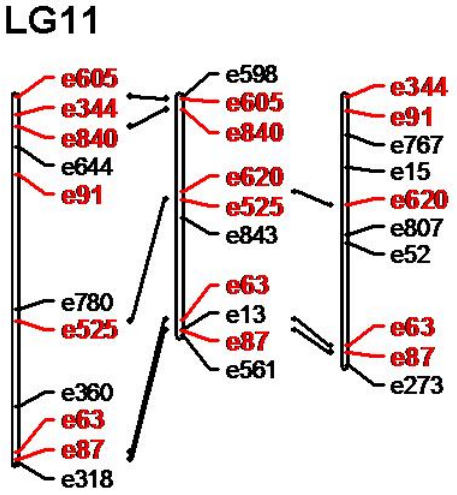
LG11
e605
e344
e840
e644
e91
e780
e525
e360
e63
e87
e318
e598
e605
e840
e620
e525
e843
e63
e13
e87
e561
e344
e91
e767
e15
e620
e807
e52
e63
e87
e273

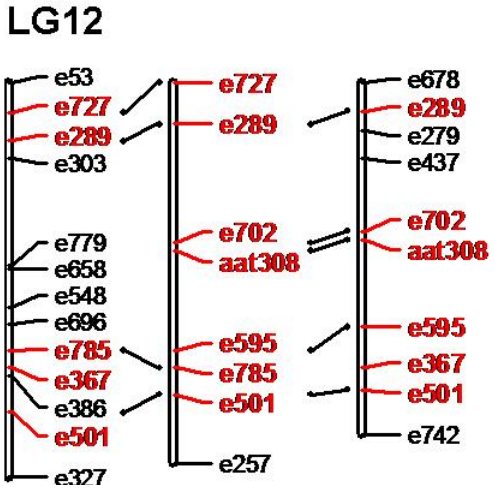
LG12
e53
e727
e289
e303
e779
e658
e548
e696
e785
e367
e386
e501
e327
e727
e289
e702
aat308
e595
e785
e501
e257
e678
e289
e279
e437
e702
aat308
e595
e367
e501
e742

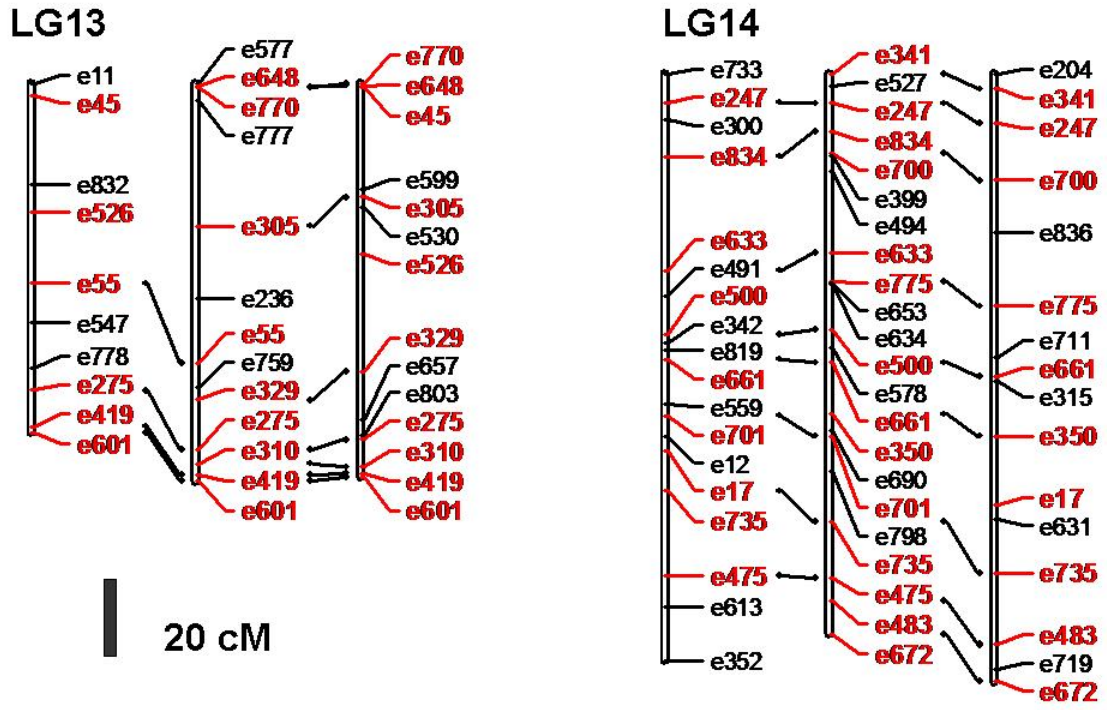

Figure 2:Three selfed F2 linkage maps of the Iron Mountain *M. guttatus* population. The three maps are shown aligned together by linkage group. From left to right: mapping population c2, c3, and c4. Marker names in black are unique to a single cross. Marker names in red are shared across at least two of the three mapping populations. Black lines connect shared markers in adjacent linkage groups (i.e. shared markers between c2 and c3, and shared markers between c3 and c4).

The initial marker screen identified 438 markers polymorphic in at least one mapping population. Of these a total of 319 markers were placed on at least one map, with 46 shared across all three maps. Any two of the three maps shared 78-87 markers, depending on the crosses. More than 2/3 of each individual map was composed of markers present in at least one other map. It is evident that the maps are almost entirely co-linear. The couple small discrepancies among closely linked markers (e.g.LG4, e234

and e498, and LG 9, e243 and e760) are probably due to genotyping error, and currently irresolvable without a higher density of shared markers or a complete genome sequence.

1.3.2 Gene based markers reveal a segregating chromosomal inversion unique to Iron Mountain

LG6 in all three maps have a region of suppressed recombination, due to a putative inversion (Figure 2). To show that this suppression is polymorphic within the Iron Mountain population, LG6 was reconstructed in an F2 population between two randomly extracted Iron Mountain inbred lines (IM179 and IM767, n=86, 19 markers) (Figure 3A). In the 179x767 population the region of suppression expanded to 40-plus cM. This region was also 40-plus cM in a *nasutus* x *guttatus* map (hereafter called SFIM) also constructed with overlapping subsets of the same gene-based markers (Figure 3A). The SFIM and 179x767 maps of LG6 were co-linear. LG6 was also collinear with SFIM and 179x767 in a perennial x annual *M.guttatus* Mgsts marker map (Lowry et al 2009) and showed no evidence of suppression (markers in the suppressed region comprised ~60 cM in this map). While definitive proof of an inversion would require cytogenetic visualization or re-construction of LG6 with the inverted ordering of markers, recombination suppression in LG6 is clearly polymorphic within Iron Mountain, and not evident in other members of the *guttatus* species complex.

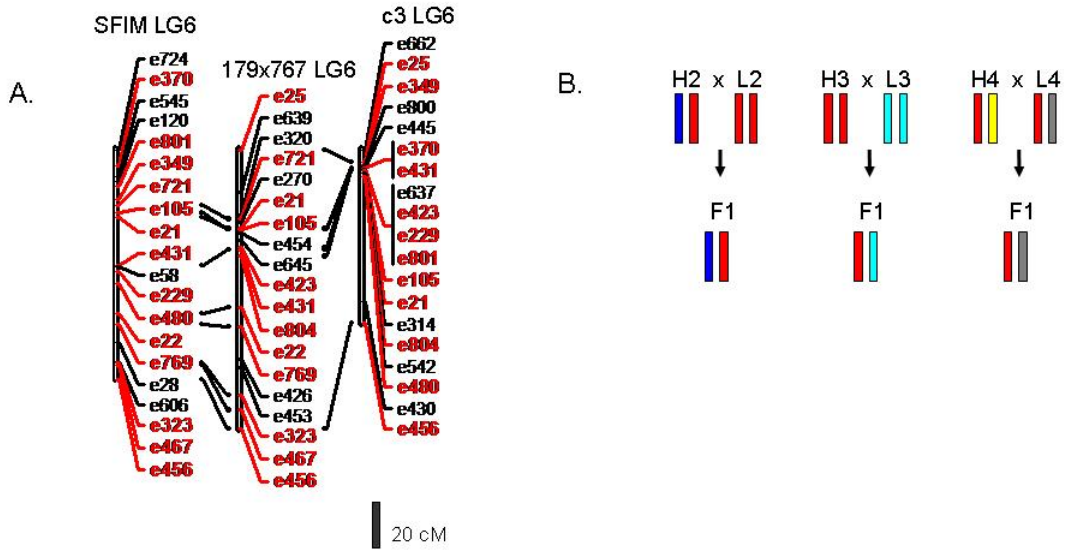

Figure 3: A polymorphic inversion in Iron Mountain. A. Comparison of LG6 marker ordering in three different mapping populations. SFIM: *M. nasutus* x annual *M guttatus*, courtesy of Carrie Wu. 179x767: two randomly extracted Iron Mountain inbred lines. c3: from Figure 1. **B**. Identification of the putative inversion haplotype by phasing parental origin of shared F1 markers. Colors indicate allele identity, e.g. L2, H3, and L3 were homozygous for all markers, L2 and H3 for the same alleles. The putative inversion haplotype alleles are indicated by red.

The three Iron Mountain F1 parents carried a common allele for every marker in the suppressed region, but not in the freely recombining region. For most of the markers we were able to phase parental origin of the F1 alleles and the common alleles were always transmitted by the same parent within each cross as one haplotype. We therefore inferred that this shared haplotype was the inversion haplotype, transmitted by the low parent in c2 and the high parents in c3 and c4 (Figure 3b). The lack of allelic

diversity within the inversion haplotype indicates that the inversion might be of recent origin.

Diagnostic markers for population sampling was identified by genotyping 96 outbred individuals one generation removed from the Iron Mountain site (no selection) for 17 gene-based markers in the LG6 suppressed region. This sample was a composite of collections from four separate years in the 1990's, and was representative of the base population for the flower size selection experiment (see Methods). We found 2 individuals entirely fixed for the putative inversion haplotype and 25 individuals that carried at least one inversion allele at each of 17 markers. We inferred that those 27 individuals carried the same inversion arrangement segregating in the F2 crosses and estimated the minimum inversion frequency in the outbred sample as (25+4)/(96x2)=15%. Alleles unique to the inversion haplotype were identified for two markers, e723 (located between e370 and e801, Lowry et al 2009) and e423 (located between e431 and e21, from scaffold 8 in the M. guttatus 7X genome). Allele 820 in marker e723 and allele 236 in marker e423 were always and only found with the inversion haplotype, and always found associated with each other. Significant LD between these two markers (D'=0.68, $p<.0001$, ns when putative inversion carriers are excluded) is unexpected given they are genetically 30-plus cM apart, and might indicate alleles captured near the inversion breakpoints. We accepted e723 and e423 together to be conservatively diagnostic for the Iron Mountain inversion haplotype.

An Iron Mountain annual population located ~50 m from the source site of our genetic studies was tested for the putative inversion in 18 wild collected individuals from 2007 with e723 and e423. We found one inversion homozygote and one inversion heterozygote (8%). We further genotyped e723 and e423 in a sample of 183 wild collected individuals from the source site in 2007, and found 27 heterozygotes and one homozygote (8%), demonstrating that the inversion allele has been maintained in Iron Mountain at appreciable frequencies over at least a ten year interval.

Two nearby populations on Cone Peak and Echo Mountain (~1 and 3 miles distant respectively) were further genotyped for the putative inversion in 24 wild collected individuals from each population. We did not find the inversion haplotype in either population (allele 820 for e723 was not detected at all). We also genotyped 24 wild collected individuals from a nearby perennial *guttatus* population on Iron Mountain to rule out introgression. We did not find the haplotype (or either diagnostic allele) in the Iron Mountain perennials. The putative LG6 inversion appears to be a recent derived mutation limited to Iron Mountain annual *guttatus*.

1.3.3 All three mapping populations are polymorphic for a verified meiotic drive locus on LG11

All parentals and F1s were genotyped for aat356, a diagnostic marker for a LG11 meiotic drive locus confirmed to be polymorphic in the Iron Mountain population (Fishman and Willis 2005, Fishman and Saunders 2008). All F1s were heterozygous for allele 180, which is associated with meiotic drive and reduced pollen fertility. aat356 is

a difficult marker to genotype due to PCR stutter and thus was not placed on the linkage maps. However e87 maps less than 0.2 cM away from aat356 and is an acceptable substitute (Fishman and Saunders 2008). The meiotic drive allele was transmitted from the high parent in all three mapping populations.

1.3.4 Transmission Ratio Distortion Loci (TRDLs)

Each marker was tested for deviation from Mendelian transmission and the p-values from were viewed in the framework of the linkage map (Figure 4). We also mapped TRDLs by implementing the multipoint Bayesian method developed by Vogl and Xu (2000). The posterior distribution of TRDL locations is presented with the posterior probabilities of TRDL detection for each linkage group (Figure 4).

Identification of TRDLs is complicated by miscoding of genotypes. In marker sparse regions spurious identification of TRDLs may result from systematic deviation from the expected segregation ratio due to difficulty in distinguishing between the heterozygote and one of the homozygote classes. Also, even when there are multiple distorted markers in a densely genotyped region, with our sample sizes the estimation of s and h for small effect TRDLs is sensitive to genotyping error in the counts of one or more of the genotype classes. This complicates the attempt to infer the mode of gene action of transmission distortion loci.

Thus TRDLs were called as significant only if they satisfied two criteria: two or more contiguously mapped markers distorted in the same direction at $p<.05$ (**)

coinciding with a peak of posterior probability of at least 5 %. Accordingly we discarded two potential TRDL peaks of >5% posterior probability in sparse regions of the map (c4, LG 3a and 4). We also discarded posterior density peaks supported by multiple contiguous markers at $p<.05$ that did not cross the 5% posterior probability threshold (c3 LG10, c4 LG1a, 3b, 8, and 13). While the selection of a 5% peak threshold is arbitrary, the double criteria employed here is conservative for the purpose of identifying loci that are distorted due to viability selection and inferring their mode of action.

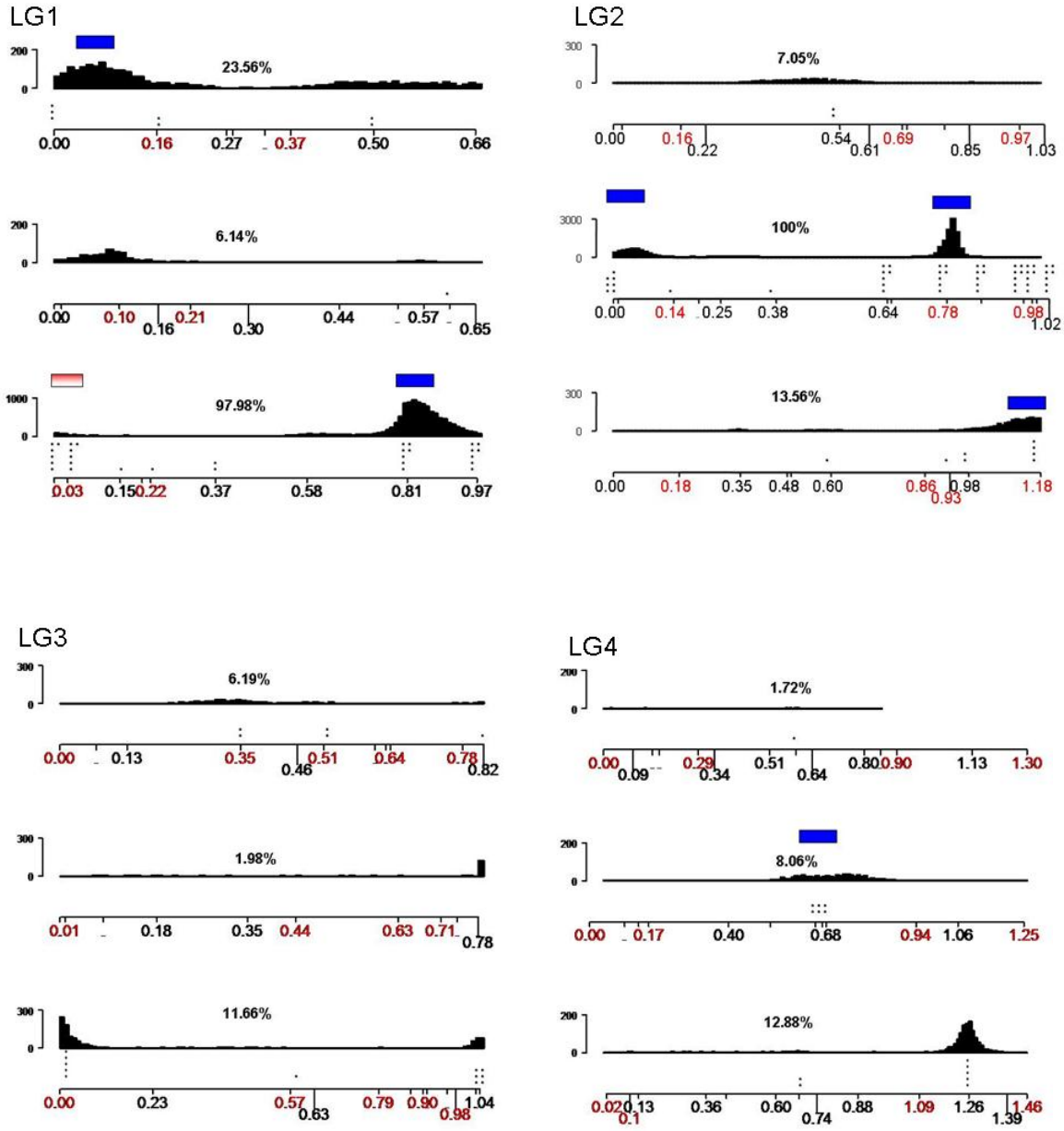
LG1
23.56%
0.00 0.16 0.27 0.37 0.50 0.66
6.14%
0.00 0.10 0.16 0.21 0.30 0.44 0.57 0.65
97.98%
0.03 0.15 0.22 0.37 0.58 0.81 0.97
LG2
7.05%
0.00 0.16 0.22 0.54 0.61 0.69 0.85 0.97 1.03
100%
0.00 0.14 0.25 0.38 0.64 0.78 0.98 1.02
13.56%
0.00 0.18 0.35 0.48 0.60 0.86 0.93 0.98 1.18
LG3
6.19%
0.00 0.13 0.35 0.46 0.51 0.64 0.78 0.82
1.98%
0.01 0.18 0.35 0.44 0.63 0.71 0.78
11.66%
0.00 0.23 0.57 0.63 0.79 0.90 0.98 1.04
LG4
1.72%
0.00 0.09 0.29 0.34 0.51 0.64 0.80 0.90 1.13 1.30
8.06%
0.00 0.17 0.40 0.68 0.94 1.06 1.25
12.88%
0.02 0.1 0.13 0.36 0.60 0.74 0.88 1.09 1.26 1.39 1.46

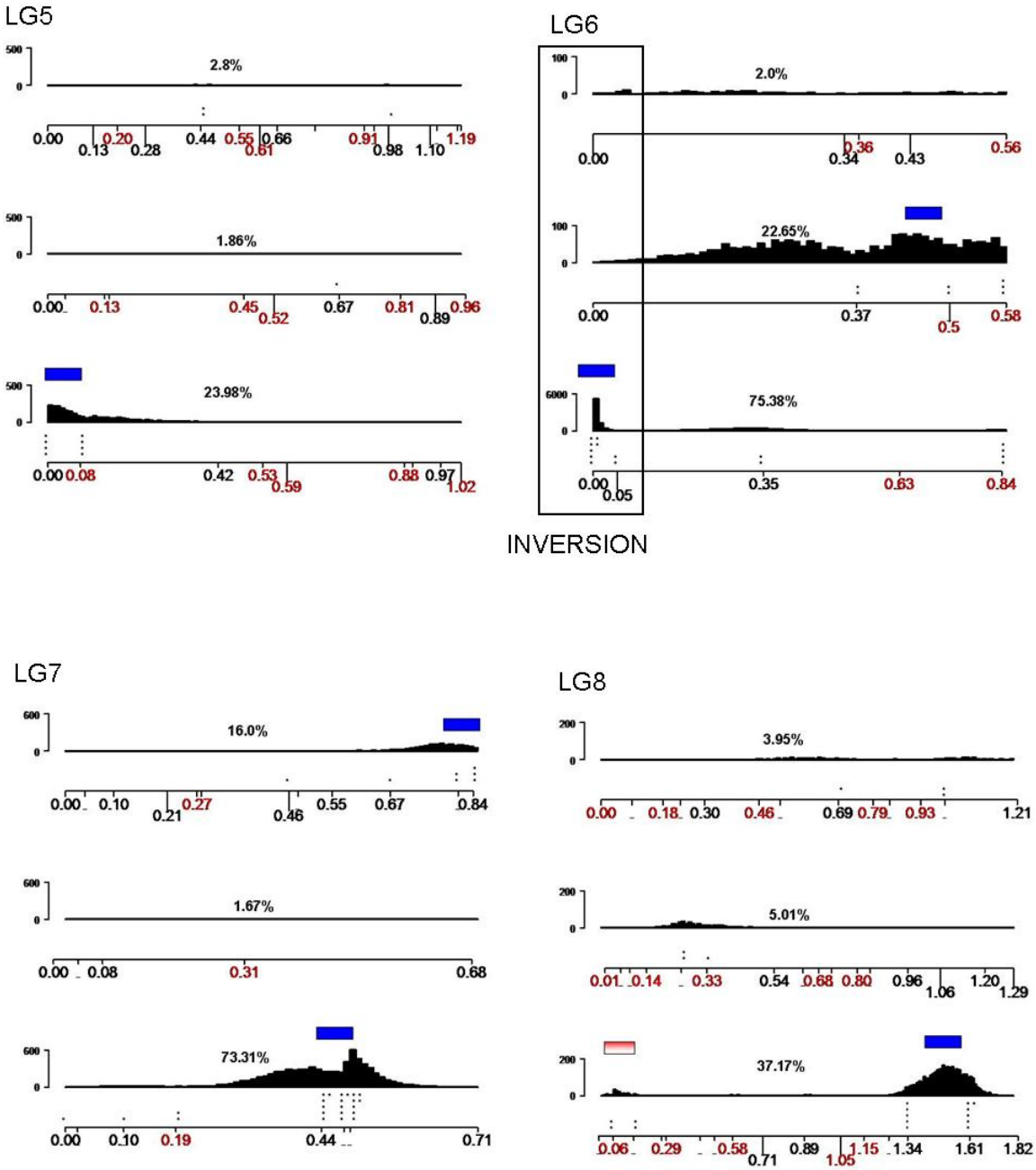
LG5
2.8%
1.86%
23.98%
LG6
2.0%
22.65%
75.38%
INVERSION
LG7
16.0%
1.67%
73.31%
LG8
3.95%
5.01%
37.17%

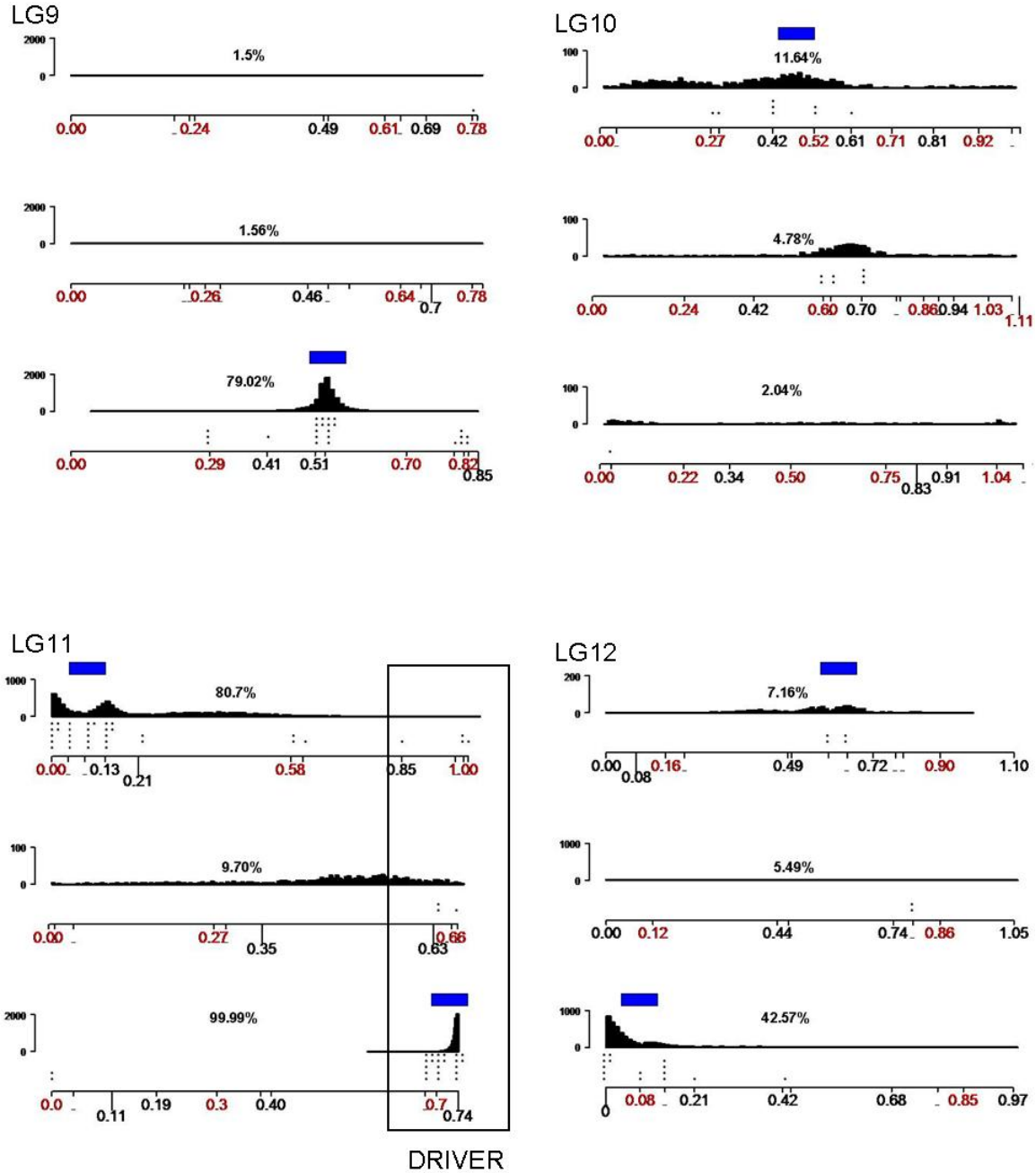
LG9
1.5%
0.00 0.24 0.49 0.61 0.69 0.78
1.56%
0.00 0.26 0.46 0.64 0.7 0.78
79.02%
0.00 0.29 0.41 0.51 0.70 0.82 0.85
LG10
11.64%
0.00 0.27 0.42 0.52 0.61 0.71 0.81 0.92
4.78%
0.00 0.24 0.42 0.60 0.70 0.86 0.94 1.03 1.11
2.04%
0.00 0.22 0.34 0.50 0.75 0.83 0.91 1.04
LG11
80.7%
0.00 0.13 0.21 0.58 0.85 1.00
9.70%
0.00 0.27 0.35 0.63 0.66
99.99%
0.0 0.11 0.19 0.3 0.40 0.7 0.74
DRIVER
LG12
7.16%
0.00 0.08 0.16 0.49 0.72 0.90 1.10
5.49%
0.00 0.12 0.44 0.74 0.86 1.05
42.57%
0 0.08 0.21 0.42 0.68 0.85 0.97

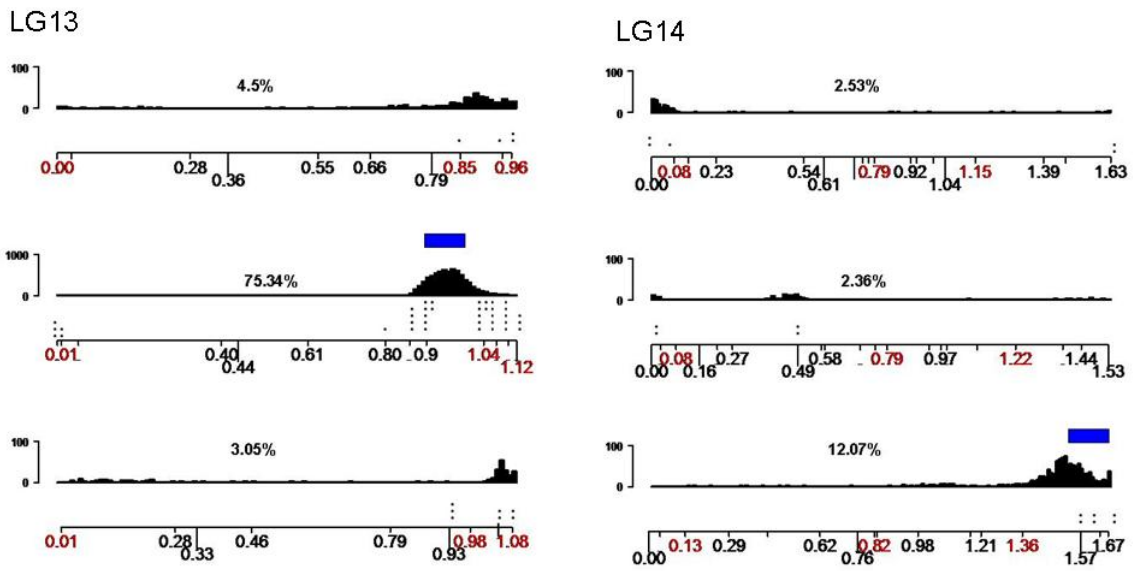

Figure 4: Transmission ratio distortion loci in 3 selfed intra-population F2 crosses. There are 14 panels, with each panel representing a linkage group, ordered from top to bottom as c2, c3, and c4. Tick marks on the x axis are marker locations in Morgans; red tick marks indicate markers shared across all three linkage maps and may be used to infer whether TRDLS mapped on the same linkage group in different crosses co-localize. P-values for chi-square tests of deviation from Mendelian expectation for each marker are indicated above its map location (*<.1, **<.05, ***<.01, ****<.001, *****<.0001, ******<.00001, ********<.000001). The y-axis are counts from the posterior distribution of TRDL locations, grouped into 1 cM intervals. Posterior frequency for TRDL detection is indicated for each linkage group. Blue bars indicate TRDLs accepted for further analysis. The two red bars indicate epistatic TRDLs (see section 1.3.6).

The Bayesian multipoint mapping method and simple identification of distorted regions based on chi-square tests were concordant. There is no instance where the Bayesian method maps a TRDL in a region without obvious segregation distortion. Where the TRDL peak was estimated as the mode of the posterior distribution, generally the most significantly distorted marker was also the genotyped marker nearest the peak location of the TRDL. The TRDLs are all unique to each cross, consistent with rare deleterious alleles. There was no bias evident in the direction of distortion; the

deleterious allele was as likely to come from the high parent as the low. In Table 2 we present a summary of the accepted TRDLs, their locations, their direction, and the genotype counts in the nearest marker.

Table 2: Summary of TRDL positions, parental origin, and associated genotype frequencies

cross	LG	TRDL peak position (cM)	parental origin of del. allele	nearest co-dom marker	nearest marker position (cM)	N ind of genotype HH	N ind of genotype HL	N ind of genotype LL	sum counts
c2	1	6.6	low	e212	0	108	193	68	369
c2	7	77.1	low	e746	80.5	105	191	67	363
c2	10	47.8	high	e27	51.7	68	171	105	344
c2	11	13.3	low	e644	9.31	126	237	3	366
c2	12	65.1	high	e548	60.4	68	193	88	349
c3	2	4.6	low	e774	0.5	122	167	91	380
c3	2	79.5	high	e274	78.1	16	249	117	382
c3	4	74.6	low	e749	66.6	100	205	72	377
c3	6	54.7	high	e430	49.6	90	169	117	376
c3	13	96.7	high	e329	89.7	69	184	130	383
c4	1	81.7	high	e757	97.1	58	178	122	358
c4	2	116.4	high	e124	104.6	79	188	113	380
c4	5	1.1	high	e417	0	67	192	117	376
c4	6	1.2	low	e431	4.5	100	196	60	356
c4	7	50.0	low	e708	49.3	123	180	62	365
c4	8	152.2	low	e333	134.2	122	155	88	365
c4	9	53.4	-	e795	52.9	118	140	118	376
c4	11	72.7	low	e87	69.8	126	204	45	375
c4	12	1.0	-	e678	0	116	141	112	369
c4	14	151.1	high	e483	156.9	68	200	99	367

1.3.5 Mode of gene action for verified TRDLs

We next inferred the mode of gene action in the accepted TRDLs (Table 3). First, we used genotype counts at TRDL markers to calculate s and h in a model of viability selection where the expected genotype ratios are 1 : 2(1-hs) : 1-s. Here h<0 indicates

overdominance, h=0 complete recessivity, h=0.5 additivity, h=1 complete dominance, and h>1 underdominance. Two TRDLs were identified as definitely underdominant (e795 and e698), where there was equal representation of either homozygotes class (thus s~0) but a clear deficit of heterozygotes. Additionally 6 estimates of h were slightly >1 or slightly <0. To determine the mode of gene action for such ambiguous loci, we calculated 95% confidence intervals for h given a model of complete dominance (h=1) and/or recessivity (h=0) for each estimated value of s(Table 3, columns h_{rec} and h_{dom}). All the ambiguous estimates of h were within the 95% confidence interval for dominant or recessive action of deleterious alleles. We also identified potentially additive TRDLs in which h was outside the range of both complete dominance and recessivity. Under the model of viability selection, when h=0.5 (additive) the expected genotype ratios are the same as that expected under gametic selection, where selection occurs in only one parent pre-fertilization. We tested the genotype counts at each locus against a model of gametic selection and indicated whether it could be rejected as a cause of transmission distortion.

Table 3: Mode of gene action for verified TRDLs.

s=selection coefficient and h=dominance coefficient in a model of viability selection. w=gametic transmission frequency for the deleterious allele in a model of gametic selection(w=0.5 under neutrality). s, h, and w were calculated from genotype counts. In h_{rec} and h_{dom} we indicate whether h is within the 95% confidence interval for h given a model of complete dominance (h=1) or recessivity (h=0) for each value of s.

cross	Lg	TRDL	s	h	h_{rec} 95% conf. interval	h_{dom} 95% conf. interval	w	test to reject gametic selection (p-value)	mode of gene action
c2	10	e27	0.35	0.53	no	no	0.39	ns	additive
c3	13	e329	0.47	0.62	no	no	0.35	ns	additive
c4	1	e757	0.52	0.52	no	no	0.32	ns	additive
c4	2	e124	0.30	0.56	no	no	0.41	ns	additive
c4	5	e417	0.43	0.42	no	no	0.36	ns	additive
c4	7	e708	0.50	0.54	no	no	0.34	ns	additive
c3	2	e774	0.25	1.24	-	yes	0.43	0.018	dominant
c3	6	e430	0.23	1.07	-	yes	0.44	0.021	dominant
c4	8	e333	0.28	1.31	-	yes	0.42	0.023	dominant
c2	1	e212	0.37	0.29	yes	-	0.39	ns	partial recessive
c2	7	e746	0.36	0.25	yes	-	0.39	ns	partial recessive
c2	11	e644	0.98	0.06	yes	-	0.02	0	recessive
c2	12	e548	0.23	-0.43	yes	-	0.44	0.048	recessive
c3	2	e274	0.86	-0.07	yes	-	0.12	0	recessive
c3	4	e749	0.28	-0.09	yes	-	0.42	0.09	recessive
c4	6	e431	0.40	0.05	yes	-	0.38	0.056	recessive
c4	11	e87	0.64	0.30	no	-	0.26	0.09	partial recessive
c4	14	e483	0.31	-0.03	yes	-	0.41	0.085	recessive
c4	9	e795	0.00	13042	-	-	-	0	underdominant
c4	12	e678	0.04	10.38	-	-	-	0	underdominant

Each TRDL's mode of gene action was determined based on the comparison of estimated h with h_{rec} and h_{dom}, as well as the test for gametic selection. 6 TRDLs were classified as "additive", where we could not reject gametic selection and h was outside of the range of both complete dominance and recessivity. 3 TRDLs were classified as "dominant" where we rejected gametic selection and h was within the range of complete

dominance. 6 TRDLs were classified as "recessive" where we rejected gametic selection and h was within the range of complete recessivity. 2 TRDLs were classified as "partially recessive" where gametic selection could not be rejected but h was within the range of complete recessivity. 1 TRDL was classified as "partially recessive" where gametic selection was marginally rejected but h was outside of the range of complete recessivity.

One of the "partially recessive" TRDL (c4 lg11) co-localizes with the meiotic drive locus (e87), but we argue that interpreting this TRDL as a viability selection locus is appropriate. While the high parent contributed the driver allele and is present in excess, the transmission advantage is significantly greater than the previously obtained measures in Fishman and Saunders 2008 (74:26 vs 58:42, Fisher's exact test p=.0258). c2 and c3 are also polymorphic for the driver, but the distortions at those loci were not severe enough to accept as TRDLs in our mapping criteria (57:43 in both cases, p=1 in Fisher's exact test with the expected 58:42, ns in the test to reject gametic selection) . The genotype proportions compared to gametic selection expectations further suggest that a mechanism in additional to meiotic drive is contributing to the c4 LG11 TRDL. A recessive deleterious allele transmitted by the low parent in addition to the driver would be consistent with the observed genotypic proportions. In this complex scenario we would tend to 1)overestimate s and 2) overestimate h as more dominant than it actually is since the expected genotypic ratios would be approximately $1 : 2(1-hs_z) - s_g : 1- s_z - s_g$,

where s_z=zygotic selection coefficient and s_g=gametic selection coefficient (s_g=.26 and.23 for c2 and c3).

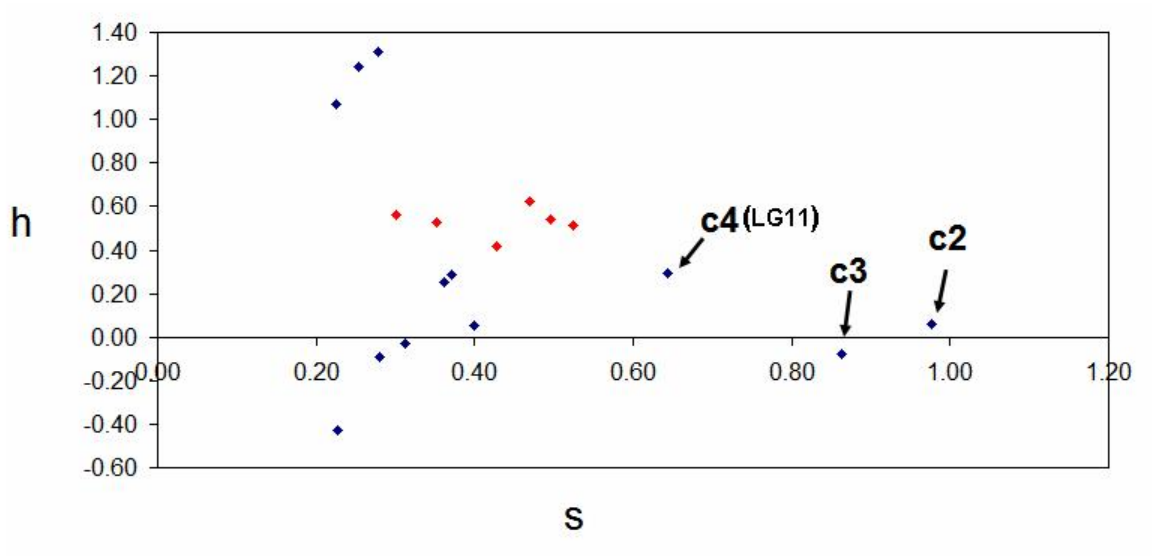

Figure 5: Relationship between effect size (s) and dominance (h) in TRDLs. Red dots indicate "additive" TRDLs, blue dots indicate the remainder. h and s are probably overestimated for the c4 LG11 TRDL (indicated by an arrow). Underdominant TRDLs were not plotted.

A clear pattern is evident in the relationship between effect size and dominance in the TRDLs (Figure 5). The distribution of dominance skews recessive (h<0.5) for the deleterious allele, with more deleterious TRDLs tending to be more recessive. Lethals (s>.8) are completely recessive (h~0) and dominant TRDLs only have minor effects. The effect size distribution for putative viability selection loci (blue dots) is bimodal, with a peak at minor effect TRDLs and a couple of lethals. We find one (or none, in the case of

c4) recessive lethals per genome, which is in the range of values for diverse animal systems in the literature (Lewontin 1972, McCune 2002).

1.3.6 Multi-dimensional epistasis contributes to transmission ratio distortion

Epistatic interaction was detected between TRDLs in mapping population c4. This population had shown markedly more distortion than c2 and c3 (Table 1) and we mapped double the number of TRDLs (Table 2). We combined 10 c4 TRDLs (Table 2) with 4 minor TRDLs that were originally discarded because they did not pass the 5% posterior probability criterion. All pairs of TRDLs were tested for non-independence of genotype proportions and 14 out of 91 pairs had p-values <0.05 (df=4), in excess of the 4 or 5 we might expect by chance. We adjusted for multiple testing with Bonferroni correction (α=0.05, p=0 .00056). Four TRDL pairs survived correction for multiple testing at α=0.06 and the p-values are presented in Table 4.

Table 4: Epistatic TRDL pairs in the c4 population. P-values in bold survive Bonferroni correction at α=0.06. P-values <.05 that did not survive Bonferroni correction are also presented. * indicates epistatic TRDLs that had not met acceptance criteria in the original multipoint Bayesian mapping analysis.

	LG9:e795	LG12:e698	LG2:e124	LG1:e827*	LG8:e227*
e795	-	**0.00063**	**0.000227**	**0.000624**	ns
e698	-	-	ns	0.001969	**0.000535**
e124	-	-	-	ns	0.003514
e827*	-	-	-	-	0.02381
e227*	-	-	-	-	-

Two definitively underdominant TRDLs , e698 and e795, had been mapped in c4 (Table 2), and both are also epistatic TRDLs (Table 4). Two minor TRDLs that had not met our acceptance criterion in Bayesian mapping were also identified as epistatic TRDLs (Table 4). These minor epistatic TRDLs are dominant or underdominant in its mode of action (Table 5). The top 6 significant TRDL pairs, 4 of which survive multiple testing, all involve combinations of the same set of 5 markers (Table 4), implying that the loci may be part of a molecular network of genes critical for embryonic viability.

The c2 and c3 TRDL pairs were also tested for non-independence, but we found no evidence of epistatic interactions. No pair of markers survived adjustment for multiple tests; c2 and c3 had only 2 and 1 TRDL pair respectively with p values <0.05.

Table 5: Mode of gene action for epistatic TRDLs of minor effect

cross	Lg	TRDL	s	h	h_{rec} 95% conf. interval	h_{dom} 95% conf. interval	w	test to reject gametic selection (p-value)	mode of gene action
c4	1	e827	0.40	0.88	-	yes	0.38	0.047	dominant
c4	8	e227	-0.07	3.57	-	-	0.52	0.0028	underdominant

1.3.7 Quantitative Trait Loci (QTLs) for male and female fertility

Each mapping population was measured for pollen viability, total pollen number per flower, and supplemented seed set per flower (Table 6). Correlation between traits was low, ranging from 4.0-48.5%.

Table 6: Summary of male and female fertility trait means and distributions. Pollen viability is % viable pollen, total pollen and supplemented seedset are counts per flower. Trait means are presented with phenotypic standard deviations.

cross	pollen viability	total pollen	supplemented seed set
c2	0.55(.17)	8597.8(3191.8)	69.2(49.8)
c3	0.48(.24)	8552.7(3849.9)	128.3(75.7)
c4	0.22(.19)	7907.2(3804.6)	72.8(64.2)

QTLs were mapped for each trait in each cross by composite interval mapping (CIM) (Zeng 1994) in QTL Cartographer (Wang et al 2007) with 5% genome wide significance thresholds determined by 1000 permutations per trait. Multi-trait composite interval mapping (MCIM) proved unhelpful due to low correlation between traits(Jiang and Zeng 1995). We do not present the CIM results here; instead we used the number of QTLs identified for each trait by composite interval mapping to define the

prior in Bayesian QTL mapping, (Yandell et al 2007) implemented in the qtlbim package in R(Yi et al 2005, 2007). It should be noted that composite interval mapping and Bayesian mapping gave concordant results, i.e. CIM QTLs were simply a subset of QTLs identified in qtlbim. Additional QTLs identified by Bayesian mapping were either epistatic loci or suggestive QTLs that had not quite met the 5% genomewide permutation threshold in CIM.

Bayesian mapping identified a total of 26 male and female fertility QTLs in the 3 mapping populations. If we take into account shared QTL across different mapping populations, 18 QTLs were identified. We present each QTL by cross, linkage group, and the marker nearest the QTL position (i.e. the mode of the posterior distribution of QTL location) in Table 7. For each QTL the genotypic means were scaled such that the low parent allele homozygotes = 0, the high parent allele homozygotes = 2a, and heterozygotes = a + d, where a=additive effect and d=dominance effect. Negative values for the additive effects indicate that the deleterious (decreasing) allele was carried by the high parent, positive values indicate that the decreasing allele was carried by the low parent. We also present the additive dominance ratio, or $d/|a|$. In this scale $d/|a|<-1$ indicates underdominance, $d/|a|= -1$ indicates complete dominance for the deleterious allele, $-1<d/|a|<0$ indicates dominance, $d/|a|=0$ additivity, $0<d/|a|<1$ recessivity, $d/|a|=1$ complete recessivity, and $d/|a|>1$ overdominance, regardless of whether the deleterious allele was carried by the low or high parent.

Table 7:Summary of QTLs for male and female fertility. pv=pollen viability, pollen=total number of pollen per flower, seed=supplemented seed set. Each QTL is identified by cross, linkage group, and nearest marker. Additive effects are presented with d/|a| in parentheses, both in units of F2 phenotypic standard deviations. QTLs in boxes (both dotted and bold) were mapped in more than one cross. The QTL in bold type – c3:LG2:e274 – is a major deleterious QTL for all three measured components of fertility as well as viability

cross	LG	pos	nearest marker	pv	pollen	seed
c2	4	102.6	e691	-0.19 (0.05)	-	-
c2	6	0	inversion	0.47 (0.97)	0.32 (0.55)	0.34 (0.95)
c2	7	41.4	e246	-0.2 (0.15)	-	-
c2	8	9.28	e178	-	-0.35 (0.01)	-
c2	11	87.4	driver	-0.28 (-0.01)	-	-
c2	14	49.8	e633	-0.05 (6.51)	-	-
c3	**2**	**78.1-80.7**	**e274**	**-0.36 (1.08)**	**-0.59 (1.34)**	**-0.63 (1.48)**
c3	6	0	inversion	-0.33 (0.03)	-	-
c3	8	9.9	e178	-	-0.19 (-0.26)	-
c3	8	99.9	e718(~e333)	-	0.34 (0.01)	-
c3	8	110.6	e472	0.38 (1.06)	-	-
c3	9	62.3-69.6	e753	0.17 (0.01)	0.24 (0.07)	-
c3	10	17.2	e846	0.19 (2.48)	-	-
c3	11	66.2-67.4	driver	-0.56 (0.63)	-0.4 (0.02)	-
c3	12	81.2	e785	-	0.01 (1058)	-
c3	13	0	e648	-	0.15 (0.88)	-
c4	4	0-6.6	e546	0.23 (0.08)	0.26 (0.02)	-
c4	6	4.5-14.8	inversion	-0.88 (-0.06)	-0.37 (0.05)	-0.44 (0.04)
c4	7	71	e746	0.17 (-0.02)	-	-
c4	8	62.3	e675	-	0.27 (0.02)	-
c4	8	134.2	e333(~e718)	-	-0.28 (-0.03)	-
c4	9	0	e536	-	-	-0.19 (0.23)
c4	10	22.3-26,9	e846	-0.2 (0.08)	-	-0.01(285)
c4	10	97.6	e465	-0.2 (0.02)	-	-
c4	11	12.7	e767	-	-	0.18 (-0.04)
c4	11	63.7-65.8	driver	-0.38 (-0.61)	-0.23 (-0.03)	-

Three overdominant loci were detected – c2:LG14:e644, c3:LG12:e785, and c4:LG10:e846. Trait means for homozygote genotypes were equivalent for these loci (i.e. additive effect ~0), suggesting that pseudo-overdominance may not explain the mode of action for these QTLs. An alternative explanation is additive-dominant epistasis (see

section 1.3.9) with an unmapped factor fixed in the background for that particular cross. True overdominance is perhaps unlikely given that all three overdominant loci are unique to single crosses (we would expect some repeat mapping if the alleles are maintained at common frequencies due to true overdominance).

There was no bias evident in the direction of fertility QTLs i.e. deleterious loci were as likely to be transmitted from the low parent as the high parent. The majority of the QTLs (12/18) were not pleiotropic for different fitness components, as expected from the low correlation between traits. The majority of QTL (13/18) were also unique to a single cross, as expected for rare deleterious loci.

The obvious exceptions to this are the segregating inversion and the meiotic drive locus. Both segregated in all three crosses, and in all three crosses affected pollen viability, in 4/6 cases affected pollen number, and of those in 2/4 cases also affected seed set. Effect size for pollen viability varied between crosses, ranging from small (0.28 sd) to major (0.88 sd). Dominance was also not consistent between crosses, ranging from dominant to completely recessive ($-1 < d/|a| \leq 1$). When an inversion allele or driver affected additional fertility traits, often the mode of gene action was not consistent (e.g. the c3 driver, which was additive for pollen number but recessive for pollen viability). Both the inversion and driver involve large regions of recombination suppression that contain Mb of genome and many genes (the meiotic drive locus expands by 20 cM in non-drive Iron Mountain crosses compared to drive polymorphic crosses, suggesting that the driver may also be captured within an inversion - Lila Fishman pers. comm.).

The contribution of these QTL alleles to trait variation in any given cross likely depends on numerous factors, including variation in coupling phase in the recombination suppressed region, variation segregating in repulsion, as well as genetic background. Despite this complexity, it seems that the inversion and driver does consistently contribute to variation in pollen viability, possibly by having captured major deleterious alleles in their recombination suppressed regions.

Where there was apparent pleiotropy in QTLs that didn't involve chromosomal rearrangements (c3:LG9:e753, c4:LG4:e546) it was between developmentally correlated traits (pollen number and pollen viability). Both these QTLs affected both aspects of male fertility similarly in terms of direction, magnitude of effect, and dominance, supporting allelic pleiotropy rather than linkage. There were also two additional QTLs (that didn't involve the driver or inversion) that were mapped in multiple crosses. Both were QTLs for pollen number (c2 and c3:LG8:e178, c3 and c4:LG8:e333).

There are several instances of co-localization between TRDLs and QTLs in c4, but this is probably not pleiotropy. We mapped TRDLs at both the inversion and driver in c4, but in both cases the deleterious alleles were transmitted from the low parent (Table 2), while the inversion and drive alleles were transmitted from the high parent. Similarly, we mapped a TRDL near c4:LG8:e333 as well as a pollen number QTL, but the deleterious TRDL allele and QTL allele was transmitted by different parents, suggesting that the co—localization is simply explained by repulsion phase linkage.

c3:LG2:e274, a major sterility QTL, co-localized with a "recessive lethal" TRDL (c3:LG2:e274, Table 2 and 3), and it is the only instance where we can infer pleiotropy between fertility and viability. The c3 population segregated in roughly Mendelian proportions (1:3) for a floral mutation that resulted in a crumpled deformed bud that often did not open, along with vegetative alterations (thickened, misshapen, brittle leaves and stems, senescing calyxes) . The population was mostly culled for the mutant phenotype as one of our goals was to measure quantitative variation in the corolla, and thus we map a major TRDL at this locus with a dearth of the HH genotype (high parent carried the deleterious allele). The deleterious genotype was not fully penetrant; 16 HH individuals made it through culling and were phenotyped (Table 2), and despite the very small sample size we map a major recessive deleterious allele for male and female fertility at this locus (deleterious allele again transmitted by the high parent).

1.3.8 Mode of action for male and female fertility QTLs

Similar to the TRDLs, a clear relationship is evident between effect size and dominance in the fertility QTLs. To view this relationship we split the fertility QTLs into two groups, pollen viability/seedset and pollen number. While there is strong selection against decreasing alleles for pollen viability and seed set, variation in absolute pollen number may actually be only loosely correlated with inbreeding depression for male fitness because pollen number per flower is very high (Table 6). For instance, a QTL of effect size 0.3 standard deviations translates into a 6-8% reduction in pollen viability or a reduction in seed set of 15-25 progeny (a significant decrease when mean seed set is 50-

75 seeds), but pollen number is reduced from a mean of ~8000 to ~7000 grains per flower, still two to three orders of magnitude greater than the average seed set. Inbreeding depression for male fertility may then be primarily driven by % pollen viability independent of pollen number, especially since there appears to be limited pleiotropy between pollen viability and pollen number (Table 7). The difference in genetic architecture evident in Figure 6 supports this view, as well as the fact that both (non-driver non-inversion) QTLs mapped in two of three crosses were pollen number QTLs (suggesting maintenance at appreciable frequencies).

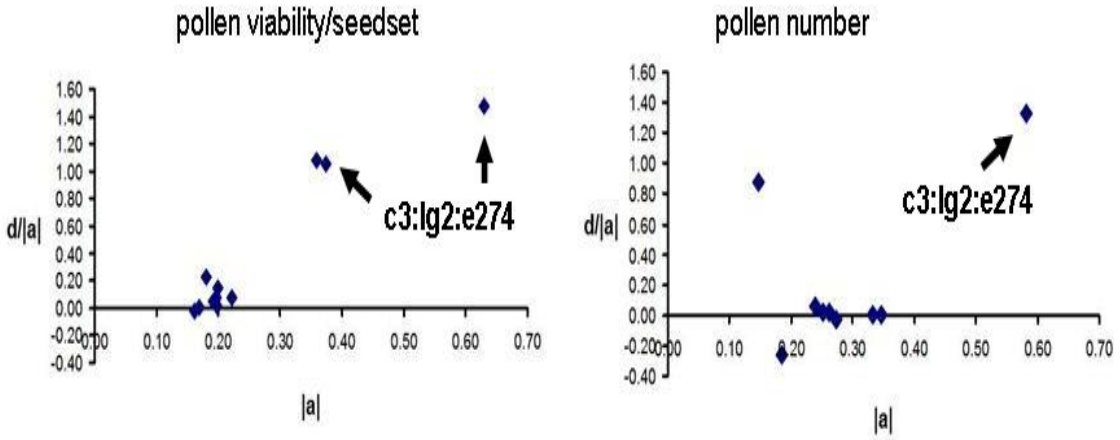

Figure 6: Mode of gene action for male and female fertility trait QTLs. The additive dominance ratio is plotted against the absolute additive effect (units in phenotypic SD). C3:LG2:e274, a major sterility locus that affected all three fertility traits, is indicated by arrows. The inversion and driver was not included in this analysis. Overdominant QTLs were also excluded.

For pollen viability and seed set, we see a bimodal distribution of effect size, with a peak of minor loci (a=0.15-0.25) and several major effect sterility loci. The minor effect loci skew recessive (d/|a|>0), and there is a clear trend in which larger effect loci are completely recessive (d/|a|~1). This is in accordance with Figure 5, where we observed the same trend and distribution with putative viability loci.

In contrast, pollen number QTLs show little evidence of a positive relationship between effect size and dominance, excluding the major QTL at c3:LG2:e274. The QTLs are larger in magnitude (a=.25-.35) and almost entirely additive. The genetic architecture of standing variation for pollen number suggests that its contribution to inbreeding depression for male fertility may be limited. The contrast in genetic architecture with pollen viability implies that selection may be acting differently on these two components of male fertility.

The inversion and drive loci were excluded from Figure 6 because of the inconsistent estimates of effect size and dominance in different genetic backgrounds. However, it is evident that both loci together explain much of the variation in male and female fertility in the F2 mapping populations. In Figure 7 we plot the percent variation explained (PVE) of F2 phenotypic variation for each pollen viability and seed set QTL against its additive effect. Given that pollen number may not greatly contribute to inbreeding depression for fertility we exclude this trait in this comparison. In Figure 7 it is evident that most of the large effect QTLs map to either the drive or inversion locus. The difference in magnitude between the inversion/drive loci and typical inbreeding

depression QTLs is remarkable when one considers that the former are known to be at common frequencies in the population while mapping results imply that the latter are rare.

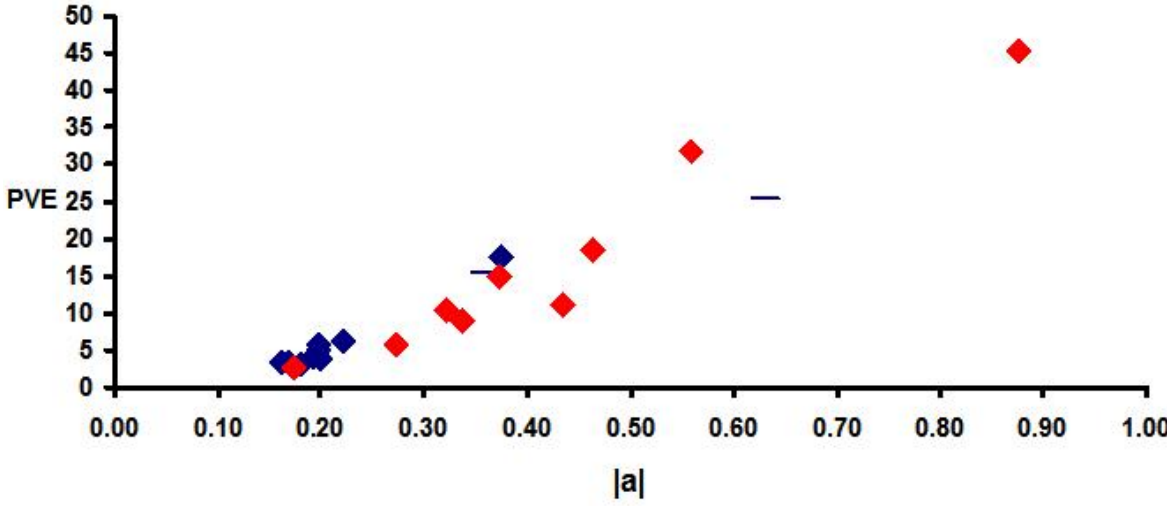

Figure 7: PVE (percent phenotypic F2 variation explained) for pollen viability and seed set QTLs. Red diamonds indicate the inversion and the drive loci, blue bars indicate the major effect sterility locus c3:LG2:e274. Blue diamonds are the remaining pollen viability and seed set loci in Table 7 (excluding overdominant loci).

1.3.9 Additive-dominant epistasis contributes to standing variation for male and female fertility

Three instances of additive-dominant epistasis were identified in two different crosses for pollen viability and seed set (Figure 8). The pollen viability interaction in c3 explained an additional 5.8 and 1.7% of phenotypic F2 variation for each interacting QTL. The estimates for PVE (percent phenotypic F2 variation explained) for the LG4 and LG12 seed set interaction QTLs were each approximately 12%, while the LG7 and

LG8 seed set interaction accounted for an additional 7.1 and 8.6 % for each QTL. These magnitudes are completely within the normal PVE range of non-epistatic QTLs for pollen viability and seed set (Figure 7).

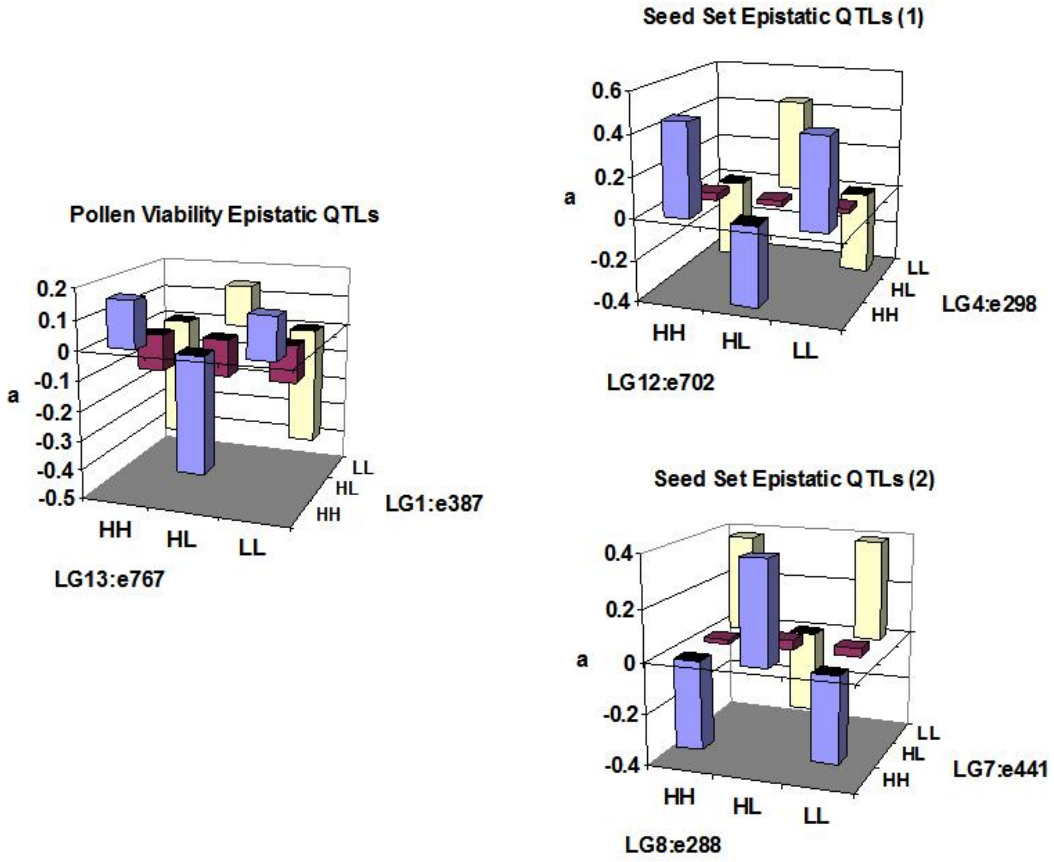

Figure 8: Additive-dominant epistasis contributes to variation in male and female fertility. The pollen viability epistatic pair was mapped in c3; both seed set epistatic qtls were mapped in c4. z-axis: 2-locus QTL genotype means (in units of phenotypic standard deviations) estimated from the posterior distribution. H and L indicate High parent and Low parent QTL alleles, respectively.

A consistent pattern is evident in the epistatic interactions. There is over or under-dominance at locus 1 given alternative homozygotes at locus 2. This results in sign epistasis at locus 2 depending on whether the genotype at locus 1 is a homozygote

or heterozygote. In this scenario we expect to observe functional overdominance and underdominance, where homozygotes have equivalently reduced or elevated fitness compared to the heterozygote. Also, this mechanism implies that in certain contexts there is no absolute directionality to purportedly "unconditional" deleterious alleles, and immediately suggests a means for the maintenance of deleterious variation through balanced polymorphisms.

1.3.10 Environment dependent epistasis for pollen viability between meiotic drive and inversion alleles

Finally, we present field data suggesting that deleterious effects may also be dependent on the environment. We had genotyped 183 wild-collected individuals from Iron Mountain in 2007 for the diagnostic inversion alleles to assess its frequency (see section 1.3.2). This 2007 collection had also been genotyped for the meiotic drive locus and phenotyped for pollen viability (see Fishman and Saunders 2008). With this dataset we confirmed that the inversion had an effect on male fertility in field collected plants ($p<.0001$, 152 non-inversion individuals and 27 inversion carriers with phenotypes) and also that the drive allele and inversion interacted in a reinforcing fashion to reduce male fertility (Figure 9). The reinforcing epistasis (see Figure 9) between drive and inversion had not been detected in greenhouse conditions, though conditions for detection were optimal: all three F2s segregated for both loci, and in c2 and c3 there was no drastic departure from mendelian segregation at either locus. The epistatic interaction thus appears dependent on field conditions. Difference between greenhouse and field

environments in QTLs for fitness related traits has been documented (Malmberg et al 2005, Weinig et al 2003). While replication of this result with larger sample sizes is desirable, it is clear that the inversion (as well as the meiotic drive locus) contributes male fitness variation on Iron Mountain in field conditions.

	df	SS	F	pvalue
drive genotype	2	0.7098	8.30	0.0004
inv genotype	1	0.8749	20.47	0.00001
drive*inv genotype	2	0.3346	3.91	0.022

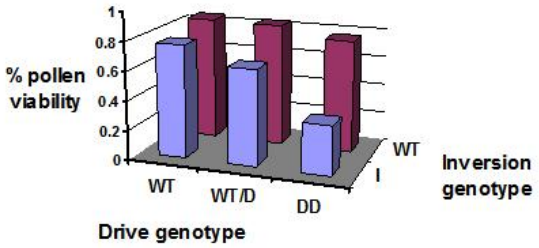

Figure 9: Environment-dependent epistasis between the meiotic drive and inversion alleles. D : driver allele, I: inversion allele. Individuals coded as "I" are all heterozygous for the inversion except for one homozygote. N=181 individuals. Above, 2-way anova for pollen viability with the inversion and drive genotypes. Below, genotypic means. The DD/I class had only 5 individuals, but was significantly different from all other 2 locus genotypes in pollen viability.

1.4 Discussion

1.4.1 Linkage map construction and identification of TRDL in the guttatus species complex

There are two previously published genetic maps within the *guttatus* species complex, an F2 cross between the perennial and annual ecotypes of *guttatus* and an F2 cross between *M. nasutus* and *M. guttatus* (Hall and Willis 2005, Fishman and Willis

2001, Fishman et al 2008). Estimated map lengths in these crosses between ecogeographic races and subspecies are ~1900 and 2092 cM respectively, comparable to that of the intra-population maps reported here, and aside from chromosomal rearrangements marker placement is generally concordant between all maps.

However, the maps estimated from intra-population crosses are clearly different from crosses between divergent groups within the species complex in terms of transmission ratio distortion. The higher-order maps had comparably more distortion than the intra-population maps (about half in both cases) and the distortion was also typically more severe compared to the standing variation. Finally, distortion was more directional between species, favoring guttatus in the *nasutus x guttatus* cross, whereas bias in the direction of distortion was not observed in the intrapopulation crosses.

The differences point to a distinct biological mechanism underlying transmission ratio distortion in within-population crosses compared to crosses between evolutionarily divergent lines. In higher order crosses the biological mechanism underlying segregation distortion is attributed to heterospecific interactions or gametophytic selection (e.g. pollen competition), especially since these crosses involved inbred lines where major lethals had already been purged (Fishman et al 2008). The larger effect sizes and directionality of transmission ratio distortion could be expected as a result of divergence time and selection. For intra-population crosses, while we cannot rule out gametic selection for 6 TRDLs with an additive mode of gene action, generally the TRDLs are attributable to seed-to-flowering viability selection on genotypes. Such loci

are expected to be generally of minor effect size and recessive for the deleterious allele, as observed.

1.4.2 Mapping suggests that both mutation selection balance and balancing selection contributes to the maintenance of fitness variation

The QTL and TRDL mapping results together indicate that deleterious variation is maintained by both mutation selection balance and balancing selection.

First, the mode of action of TRDLs and QTLs for viability and fertility suggests that mutation selection balance of deleterious mutations results in inbreeding depression by dominance exactly as expected for the majority of deleterious loci. There is no a priori expectation that new input of deleterious mutation is recessive, in fact a mutation accumulation experiment, coupled with crosses to estimate the dominance of new mutations, suggests that the dominance of new mutations ranges across the full spectrum of dominant to recessive (Shaw and Chang 2005). Thus, the recessive skew of standing deleterious variation with larger effect sizes points to the continual input of variation by mutation, and subsequent removal by selection, resulting inbreeding depression of fitness-associated traits with selfing. This result is consistent with the conclusions of Willis 1999 a,b, and c.

However, the inversion and drive loci, with their consistent effects on male fitness, suggest that a subset of deleterious variation is partly maintained by selection. This is consistent with the results of Kelly 2003. Deleterious pleiotropic effects seem to be hitchhiking along due to recombination suppression in these genomic regions, and as

a result can be maintained at intermediate frequencies. The selection can be internally driven a la the drive locus on LG 11 (Fishman and Saunders 2008). But there is no evidence of such internally driven mechanisms for the segregating inversion allele, suggesting that deleterious mutation could also be maintained by ecological selection. Given the observation of reinforcing epistasis between these two loci and the intermediate frequencies of the drive locus, the maintenance of the inversion at appreciable frequencies is quite interesting. We surmise the involvement of a tradeoff where the positive effects of early flowering is offset by the deleterious effects on male fitness (Scoville et al 2009 demonstrated that the inversion contributed significantly to population level genetic variance for flowering time). As we have a simple diagnostic method for the inversion, we should be able to test specific theories as to its maintenance by selection in experiments on the source site on Iron Mountain.

The inversion and drive loci are genomic oddities with major effects on male fertility that can be easily detected. But, in principle, hitchhiking of deleterious mutation and their maintenance by selection can be happening at the genic level as well among closely linked mutations. This is perhaps even likely given high deleterious mutation rate estimates (Mukai 1972, Keightley and Walker 1999) especially for traits closely affecting fitness like viability (Houle 1992, Houle et al 1996). That a subset of deleterious mutation may be maintained at common frequencies is perhaps also consistent with molecular population genetics studies that showed a signature of interference by deleterious mutations in linkage to selected sites (e.g Betancourt and

Presgraves 2002). Evidence for the maintenance of deleterious mutation at intermediate frequencies , perhaps by balancing selection, has also been demonstrated for female fecundity in Drosophila (Charlesworth et al 2007). Evidence that positive selection shapes variation in fitness components is also seen in Gardner et al 2005, in which the viabilities of wild-extracted Drosophila chromosomes were shown to be replicable in its fluctuations (this was without inbreeding).

Further, additive dominant epistasis suggests another mechanism for the maintenance of deleterious variation. It is evident that additive dominant interactions involve over/underdominance at one locus and sign epistasis at the other; the deleterious effects of genotypes are context dependent. In such a two locus system we would expect resistance to purging of deleterious variation (Byers and Waller 1999) , and perhaps maintenance of a balanced polymorphism. Signature of balancing selection at a locus exhibiting sign epistasis for growth rate has been documented in Arabidopsis (Kroymann and Mitchell Olds 2005).

1.4.3 Implications of epistasis for relevance of standing variation for adaptation

Modification of deleterious effects depending on genetic background and environmental conditions suggests that to some extant, "unconditional" deleterious variation may be context dependent. This has implications for the relevance of standing variation for adaptation. Could something like the inversion actually fix given the right genetic and environmental context? The apparent malleability of "deleterious" and "beneficial" categories for mutations suggests that even standing variation that we

would normally discount could actually be relevant for adaptation given the right context. This empirical observation is consistent with the recent interest in "soft sweeps"(Barrett and Schluter 2008) and models of adaptation from the standing variation (Hermisson and Pennings 2005, Orr and Betancourt 2001).

1.4.4 Implications of epistasis and environmental dependence for the evolution of selfing

The resistance to purging as a result of additive dominant epistasis would promote outcrossing. But what would happen in conditions that promotes the evolution of selfing – small isolated populations in novel environments? Exploration of genotypic space through selfing could result in novel favorable gene combinations that move the trait beyond the progenitor population mean while quickly purging unfavorable combinations (Charlesworth 1992, Holeski and Kelly 2006). In this case we would expect to see epistatic QTL combinations in QTL studies between evolutionarily divergent lines particularly if selfers were involved. and perhaps also in the genetic architecture of domestication events where variation is bottlenecked (e.g. Lukens and Doebley 1999, Carlborg et al 2006). Few studies look at epistasis because until recently there were many technical limitations in terms of genotyping, sample size, and also computation, but there is increasing awareness that epistasis should be taken into account (Carlborg and Haley 2004, Phillips 2008, and Malmberg and Mauricio 2005).

1.4.5 Implications of epistasis for the dominance and overdominance hypotheses

TRDL and QTL analysis both show that the dominance of loci can be modified by segregation of additional loci in the background. This has implications for the genetic basis of heterosis, a classic unresolved conflict between two distinct hypotheses. Heterosis and the sustained response to selection for yield increase may be at least partly explained by additive-dominant epistasis. Increasingly sophisticated crossing experiments explicitly designed to detect epistasis (e.g. Radoev et al 2008, Franco Garcia et al 2008) find a role for epistasis in explaining heterosis.

1.4.6 Conclusions

Inbreeding depression is explained by both mutation selection balance and maintenance of some deleterious mutation by selection. In addition, additive dominant epistasis may contribute to deleterious polymorphisms being maintained through balanced polymorphisms. The categories of beneficial and deleterious for the fitness effects of mutations are malleable due to epistasis, with implications for the relevance of standing variation for adaptation, the fate of small populations, the evolution of selfing, and the harnessing of heterosis for crop improvement

2. Standing variation for floral morphology, leaf size, and time to flowering in a natural population of common monkeyflower *(Mimulus guttatus)*

2.1 Introduction

Recent developments in genomic resources, together with the framework of quantitative population genetics, provide evolutionary geneticists with an unprecedented opportunity to address questions regarding natural variation in complex traits. These classic topics of investigation include the genetic basis of variation for a complex trait within a population, the evolutionary processes that maintain the variation, and the contributions of standing genetic variation to phenotypic diversification and adaptation at higher levels of divergence.

Variation is ubiquitous at every level of phenotypic expression (Darwin 1859, Lewontin 1974, Olesiak et al 2002). Appreciable heritabilities are estimated for almost any trait in natural populations as well as experimental laboratory populations (Houle 1992). There are also immense amounts of variation in both sequence and structural arrangements within populations (Haldane 1932, Li 1996, Tuzun et al 2005). Intra-population polymorphism at some subset of the genomic variation must underlie the quantitative trait variation, but the role of selection in maintaining polymorphism is unclear.

Models of the maintenance of standing genetic variation can be classified into two categories that differ on the role of selection. In **mutation –selection hypotheses**, heritability reflects a balance between mutation that introduces variation and (apparent)

stabilizing selection that depletes the variation. (Lande 1975, Barton 1990, Keightley and Hill 1990, Zhang et al 2004, Zhang and Hill 2005,). **Balancing selection hypotheses** propose that selection maintains trait variation. There are numerous mechanisms that lead to this result: simple overdominance, polygenic overdominance (Gillespie and Turelli 1989) frequency-dependent selection, overdominance induced by antagonistic pleiotropy (opposing effects on different fitness components - Rose 1982, Hedrick 1999), and variable selection on genotypes in spatially and temporally heterogenous environments, perhaps due to gene-environment interactions (GEI), resulting in marginal overdominance when summing over numerous environments (Levene 1953, Hedrick et al 1976, Hedrick 1986).

If heritability is maintained by balancing selection, there are two general predictions from the theory. First, polymorphisms at intermediate, sometimes stable frequencies are expected under balancing selection, while polymorphisms are expected to be mostly rare if selection is purifying. Second, the most general feature of balancing selection models is marginal overdominance. The empirical data that corresponds to these two theoretical expectations is largely absent for complex traits, due to the quantitative nature of such variation (Lewontin 1974). Any phenotypic value has a heterogeneous genetic basis and the effect of a particular allele substitution is small relative to the genetic and environmental variance, so we cannot assign genotypes to observed phenotypes. Identifying loci underlying variation in a quantitative trait was

regarded as an almost impossible task and the joint distribution of allele frequencies and trait/fitness effects for each locus underlying the trait was considered unmeasurable.

Recent developments in genomic resources and genotyping technology have placed the Mendelization of a complex trait within reach. Indeed it has become unexceptional to identify QTLs (genomic regions encompassing 10-30 cM) associated with variation in complex traits in non-model systems. The scale of the effort required for genetic dissection should not be underestimated – defining the allele, the segregating unit underlying any given QTL, will likely require some combination of positional cloning and LD mapping for each locus (e.g. Colosimo et al 2005), and we are a long ways from a general understanding of the genetic composition of a quantitative trait in any model system. However the detection of marginal overdominance, together with an understanding of the environmental conditions that result in such heterozygote advantage, and intermediate allele frequencies, will be a significant indicator that selection actively contributes to the maintenance of standing variation for that trait (Lewontin 1974). Thus the role of selection in shaping segregating variation may be effectively addressed by focused study of a few points in the total distribution of alleles.

There are numerous examples in the genetic model system *D. melanogaster* where segregating alleles have been defined by association or LD mapping (e.g. Lyman and Mackay 1998, Long et al 1998 and 2000, Lyman et al 1999, Robin et al 2002, Carbone et al 2006). Although replicating the results obtained in isogenic inbred lines in wild-caught cohorts has proved difficult (bristle number, Genissel et al 2004, MacDonald and Long,

2004), there are also successes (bristle number, MacDonald et al 2005, wing shape, Dworkin et al 2005). Some of these alleles were at intermediate frequencies; in one case the pattern of molecular variation around the locus was consistent with balancing selection (Carbone et al 2006). The obvious limitation is that the ecology of fruitfly is obscure and the fitness of genotypes is difficult to assess in the field. All the core genetic model systems where genetic dissection is most feasible share the same lack of an ecological context.

We present here a study of the genetic basis of standing variation for flower size in a natural population of common monkeyflower. This is a study system which unites ecological context for the trait examined with tractability for genetic dissection and the ability to assay genotypes for trait and fitness effects in field conditions. Significant additive and non-additive genetic variation has been shown to be present within the Iron Mountain population for both floral and fitness traits (Kelly and Arathi 2003). Quantitative genetic experiments have demonstrated that deleterious alleles (presumably rare and recessive) contribute to, but are not sufficient as an explanation for observed levels of variation in flower size and also implicated epistasis (Kelly and Willis 2001, Kelly 2003). The rejection of the deleterious mutation model (Kelly and Willis 2001) suggests that some of the variation for flower size could be due to common alleles maintained by balancing selection.

2.2 Materials and Methods

2.2.1 The study system: a variable population in a heterogeneous and extreme environment

The Iron Mountain annual monkeyflower population is a north facing alpine xeric meadow at elevation approximately 4200 ft. *M. guttatus* on this site are annuals, germinating before winter or during the spring thaw and bolting after snowmelt in late May/early June. Individuals typically produce one flower and die of desiccation. The growing season is short and extreme, starting at snowmelt in late May-early June and ending mid July when the soil is completely dry (Figure 10). Water availability over the course of the six week growing season depends almost entirely on snowmelt: the 30 year daily rainfall averages, taken at Santiam Junction (16 miles distant) ranges from 10/100 to 3/100 inches from June 1 to July 15 (from the National Climate Data Center).

June 6 2007 June 25 2007 July 15 2007

Figure 10: Extreme conditions define the growing season for the Iron Mountain monkeyflower population.

In addition to the extreme conditions book-ending the growing season, there is fine scale spatial heterogeneity for water supply, the most obvious candidate for a selective agent. For instance, the water supply is longer lasting in the shade near the tree line, such that plants near the tree line often survive a week or longer (Figure 11). In addition to spatial heterogeneity in water supply, there is temporal heterogeneity in pollinator availability. In 2007 all pollination occurred in a discrete one week period in late June-early July, and there was no pollination observed before or after that period (pers.obs.).

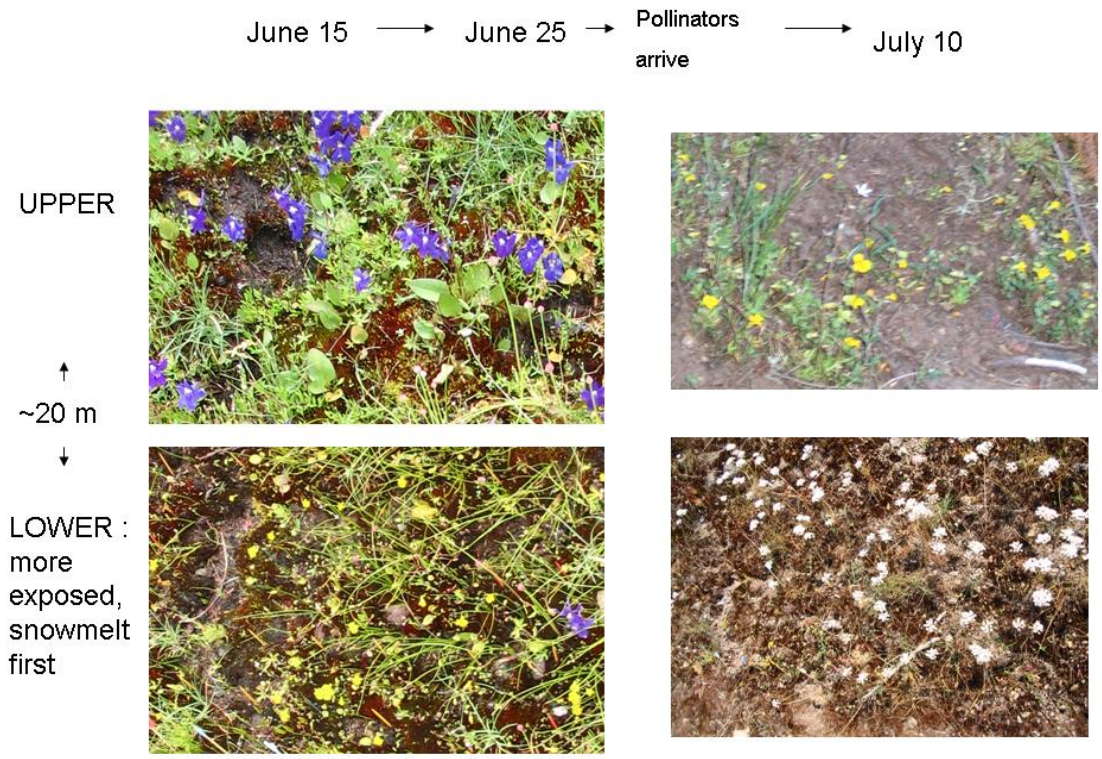

Figure 11: Heterogeneity in environmental conditions on Iron Mountain in the 2007 growing season. Time is on the horizontal axis, space on the vertical axis. In mid June, the lower slope was in full flower while the upper slope is just beginning to bolt. The water supply defines the length of the growing season. By mid July, all plants in the lower slope are dead, but plants survive near the tree line in the upper slope.

2.2.2 Phenotypic measurements on morphological traits

All individuals in the c2, c3 and c4 mapping populations (see section 1.2.2) were phenotyped on the first and second flowers of each plant for the following morphological traits in units of 1/100 inches: flower width, flower length, pistil length, and stamen length, as well largest leaf width at anthesis. These traits were measured in addition to the fertility components (estimated on the first to fourth flowers, section 1.2.4). These are standard traits in the study of trait divergence in this species complex and have been measured in other higher order crosses (Fishman et al 2002, Hall and Willis 2005). In addition to the morphological traits we noted the day of flowering and calculated time to anthesis as days since seeding. As the suite of morphological traits and fertility components (from chapter 1) were measured in the same experiment, we were able to do a straightforward comparison of genetic architecture between those two trait categories.

2.2.3 Quantitative Trait Locus (QTL) mapping

Mapping procedures were the same as detailed in section 1.2.3 and 1.2.8.

2.2.4 Comparison with divergent QTLs

QTLs affecting the same set of traits as listed in section 2.2.2 were mapped in a set of recombinant inbred lines (RILs) between Dun, a coastal perennial *guttatus* ecotype, and IM62, an inbred line derived from Iron Mountain. The linkage map construction for this population is detailed in Lowry et al 2009. Briefly, 172 advanced generation

recombinant inbred lines segregating for Dun and IM62 alleles as well as the two cytoplasms were genotyped for 239 markers. We grew 3-7 replicates of each line in a greenhouse phenotyping experiment in standard well-watered conditions and mapped QTLs on the trait averages of each RIL.

2.3 Results

2.3.1 Quantitative Trait Loci (QTLs) for standing variation in floral morphology, leaf size, and flowering time on Iron Mountain

The c2, c3, and c4 populations were phenotyped for the traits relevant to mating strategy and viability in field conditions. The traits included aspects of floral morphology, time to anthesis, and a measure of vegetative vigor (largest leaf width at anthesis) (Table 8). All traits were normalized through square root, log, or boxcox transformation, and standardized for mapping (Sokal and Rohlf 2000).

Table 8: Phenotypic means and distributions of F2 of ecologically relevant traits in the F2 mapping populations. All measures are in 100th inch, except for anthesis which is in days since seeding. Phenotypic standard deviations are presented in parentheses. cw=corolla width, cl= corolla length.

cross	cw	pistil	cl	stamen	anthesis (days)	leaf width
c2	60.7(9.4)	51.5(4.8)	73.5(8.9)	41.2(3.6)	29.4(2.9)	50.6(15.4)
c3	58.3(9.5)	49.8(4.5)	67.5(8.3)	39.4(3.1)	30.3(3.5)	64(14.7)
c4	65.4(12.4)	55.1(5.2)	82.8(11.0)	43.9(4.1)	30.2(3.7)	56.7(14.2)

QTLs were mapped for each trait in each cross by composite interval mapping (CIM) (Zeng 1994) in Windows QTL Cartographer (Wang 2007) with 5% genome wide significance thresholds determined by 1000 permutations per trait. Phenotypic trait correlations between morphological traits were significant and higher than that between fertility components, ranging from 0.6 to 0.8. However, lability in the trait correlations resulted in mixed success with MCIM mapping (Jiang and Zeng 1995). CIM results indicated that there were numerous QTL peaks that affected just one floral component. This, combined with the polygenic nature of all traits with QTLs distributed on all linkage groups, resulted in MCIM peaks that were difficult to interpret (see section 1.2.8).

QTLs identified for each trait by CIM defined the prior in Bayesian QTL mapping, (Yandell 2007) as implemented in the qtlbim package in R. As with the fertility components, composite interval mapping and Bayesian mapping gave concordant results. Additional QTLs identified by Bayesian mapping were either epistatic loci or suggestive QTLs that had not quite met the 5% genomewide permutation threshold in CIM. MCIM results were used to guide the identification of pleiotropic QTL (e.g. MCIM results sometimes guided the selection of expanded models to compare to the "best" models estimated from the Bayesian posterior). We present in Table 9 Bayesian mapping results for each of 3 F2 mapping populations.

Table 9: Summary of QTLs for floral components, leaf width, and flowering time. The QTLs are organized by cross, and then by trait. For each QTL the additive effect *a* is reported with the additive-dominance ratio $d/|a|$ in parentheses. Positive estimates of a indicate that the high parent carried the increasing allele, negative values indicate that the high parent carried the decreasing allele. Interpretation of $d/|a|$ is as follows: $d/|a|<-1$ underdominant i.e. hets have smaller trait values than the homozygotes, $-1 \leq d/|a| <0$ dominant for the decreasing allele (recessive for increasing allele), $d/|a| = 0$ additive, $0 < d/|a| \leq 1$ dominant for the increasing allele (recessive for decreasing allele), $1 < d/|a|$ overdominant i.e. hets have larger trait values than homozygotes. All units are in F2 phenotypic standard deviations. Pos=linkage map position in cM, marker=closest genotyped marker, cw=corolla width, cl=corolla length, ft=flowering time. Dotted boxes indicate shared corolla width QTL. Red boxes indicate variation in dominance in putatively pleiotropic loci.

cross	lg	pos	marker	cw	cl	pistil	stamen	ft	leaf	traits
c2	4	130	e817	0.31 (-0.02)	-	-	-	-	-	corolla
c2	11	74	e360	-	-	0.3 (0.01)	-	-	-	pistil
c2	12	0	e53	-	-	0.23 (-0.03)	-	-	-	pistil
c2	10	35	e463	-	-	-	0.43 (-0.02)	-	-	stamen
c2	14	94	e701	-	-	-	0.24 (-0.01)	-	-	stamen
c2	8	77 - 82	e31	0.21 (0.04)	-	-	0.22 (0)	-	-	flower
c2	10	47 - 56	e27	-	0.27 (-0.02)	0.25 (-0.05)	-	-	-	flower
c2	14	0	e733		0.24 (0.01)	0.22 (0.02)	-	-	-	flower
c2	1	56 - 61	e757	-	0.28 (-0.02)	0.24 (0.01)	0.28 (-0.01)	-	-	flower
c2	2	103	e831	0.3 (-0.07)	0.21 (-0.08)	-	0.23 (-0.11)	-	-	flower
c2	13	18 - 22	e832	0.36 (0.02)	0.25 (0.28)	-	0.33 (0.15)	-	-	flower
c2	14	75 - 77	e819	0.38 (0.01)	0.31 (0.06)	0.25 (0.07)	-	-	-	flower
c2	4	17	e219	-	-	-	-	0.23 (-0.01)	-	anthesis
c2	5	4	e649	-	-	-	-	0.33 (-0.05)	-	anthesis
c2	5	85	e676	-	-	-	-	0.23 (0.31)	-	anthesis
c2	8	9	e178	-	-	-	-	-0.22(-0.05)	-	anthesis
c2	8	18	e610	-	-	-	-	-	-0.3 (-0.02)	leaf
c2	9	4	e536	-	-	-	-	-	0.34 (1.22)	leaf
c2	10	42	e321	-	-	-	-	-	-0.21 (0.08)	leaf
c2	12	53	e658	-	-	-	-	-	0.2 (0.01)	leaf
c2	14	104	e17	-	-	-	-	-	0.25 (-0.02)	leaf
c2	2	72 -78	e461	0.27 (-0.12)	-	-	-	0.29 (0.01)	0.22 (-0.39)	whole plant
c2	6	0	INV	0.23 (0.71)	0.38 (0.85)	0.3 (1.19)	0.48 (0.67)	-0.2 (0.04)	0.33 (0.81)	whole plant

cross	lg	pos	marker	cw	cl	pistil	stamen	ft	leaf	traits
c3	9	0	e416	0.18 (-0.03)	-	-	-	-	-	corolla
c3	10	94	e109	0.26 (0.1)	-	-	-	-	-	corolla
c3	13	72	e55	0.3 (0.01)	-	-	-	-	-	corolla
c3	14	122	e735	0.21 (0.03)	-	-	-	-	-	corolla
c3	8	10	e278	0.25 (-0.52)	-	-	-	-	-	corolla
c3	8	57	e590	-	0.4 (-0.01)	-	-	-	-	corolla
c3	8	129	e829	-	0.26 (0.02)	-	-	-	-	corolla
c3	7	45	e512	0.42 (0.02)	0.44 (0.03)	-	-	-	-	corolla
c3	1	51	e665	-	-	0.2 (-0.01)	-	-	-	pistil
c3	3	39	e581	-	-	-0.24 (0.02)	-	-	-	pistil
c3	5	58	e176	-	-	-0.36 (-0.01)	-	-	-	pistil
c3	7	12	e259	-	-	0.28 (-0.02)	-	-	-	pistil
c3	10	109	e837	-	-	0.25 (0.09)	-	-	-	pistil
c3	12	55	aat308	-	-	0.47 (0.01)	-	-	-	pistil
c3	9	58	e371	-	-	-	0.2 (0.02)	-	-	stamen
c3	1	25	e781	-	-	-	0.21 (-0.07)	-	-	stamen
c3	2	81	e274	-	-	-	-0.24 (0.68)	-	-	stamen
c3	7	22	e34	-	-	-	0.31 (-0.04)	-	-	stamen
c3	6	21-25	e541	0.3 (-0.05)	0.3 (0.01)	0.32 (0.05)	-	-	-	flower
c3	8	113	e294	0.25 (0.04)	-	0.31 (0.1)	-	-	-	flower
c3	13	53	e236	-	0.29 (0.01)	-	0.3 (0.09)	-	-	flower
c3	6	0	INV	-	-	-	-	0.4 (-0.01)	-	anthesis
c3	9	9	e536	-	-	-	-	0.22 (0.01)	-	anthesis
c3	2	96-102	e831	0.27 (0.04)	0.28 (0.01)	0.23 (0.06)	0.25 (0.36)	-	0.26 (0.01)	whole plant
c3	11	47 -53	DR	-0.24 (0.02)	-	-	-0.3 (-0.01)	-	-0.31 (0.18)	whole plant
c3	1	65	aat225	0.27 (-0.02)	0.29 (-0.01)	-	-	-0.15 (-0.2)	0.2 (0.02)	whole plant
c3	4	101-10	e94	-	-	-	0.27 (-0.03)	0.23 (0.28)	0.31 (0.01)	whole plant
c3	5	0 - 8	e649	0.19 (0.01)	-	0.41 (0.02)	0.27 (0.04)	0.41 (-0.01)	0.29 (0.01)	whole plant
c3	8	74-80	e842	0.36 (-0.02)	-	-	0.3 (0.02)	0.32 (0.01)	0.32 (-0.01)	whole plant

cross	lg	pos	marker	cw	cl	pistil	stamen	ft	leaf	traits
c4	6	0	INV	0.24 (0.01)	-	-	-	-	-	corolla
c4	8	69	e30	0.35 (0.09)	-	-	-	-	-	corolla
c4	9	70	e753	0.18 (-0.07)	-	-	-	-	-	corolla
c4	14	74	e711	0.31 (0.01)	-	-	-	-	-	corolla
c4	11	62	DR	-	0.27 (-0.01)	-	-	-	-	corolla
c4	6	21	e28	-	-	0.05 (8.23)	-	-	-	pistil
c4	2	52	e56	-	-	-	-0.2(0.06)	-	-	stamen
c4	13	16	e599	-	-	-	-0.27(0.01)	-	-	stamen
c4	13	95	e803	-	-	-	-0.26(0.19)	-	-	stamen
c4	7	54-58	e708	0.23 (0.01)	-	-	0.29 (-0.01)	-	-	flower
c4	1	31-33	e271	-	0.24 (-0.01)	0.22 (0.02)	-	-	-	flower
c4	11	51	e52	-	-	0.25 (-0.02)	0.2(-0.14)	-	-	flower
c4	3	27-34	e429	-	-0.27 (0.48)	-0.27 (-0.02)	-0.31(0.31)	-	-	flower
c4	10	42-50	e27	0.42 (-0.62)	0.54 (-0.5)	0.61 (-0.52)	0.42(-0.15)	-	-	flower
c4	4	136-41	e573	-0.35 (0.84)	-0.47 (0.98)	-0.37 (0.95)	-0.42(0.86)	-	-0.5(1.28)	whole plant
c4	10	98-100	e754	0.27 (0.04)	-	-	0.23(0.03)	-	0.22(0.08)	whole plant
c4	13	52-58	e526	-	-0.33 (0.01)	-0.31 (-0.03)	-	-	-0.19(0.08)	whole plant
c4	5	92-97	e682	-	-	-	-	-0.23(-0.49)	-0.2(0.01)	whole plant
c4	1	15-24	e287	0.21 (-0.04)	-	-	0.27(0.01)	0.35(0.01)	0.34(0.01)	whole plant

We summarize general patterns evident from the reported QTLs in Table 9.

2.3.1.1 Artificial selection for corolla width was effective.

All but one of the flower size QTLs are in the right direction (i.e. high parent carried the increasing allele). There are two exceptions, the c3 drive locus and c4:LG4:e573, a highly pleiotropic QTL in the wrong direction. The drive locus is subject to forces other than the artificial selection imposed by the experiment and we do not consider it further. As one might expect c4:LG4:e573 exhibits complete dominance (i.e. absolute value of $d/|a|$ is near 1). Such a QTL would not respond to selection in our outbred scheme and would be revealed only in the selfed F2, and this probably accounts for the wrong direction of the QTL despite its comparatively large effect.

2.3.1.2 Genetic basis of the correlated response to selection for corolla width

Numerous QTLs for traits other than flower size are in the wrong direction (in increasing order of proportion wrong direction QTLs, corolla length, pistil length, stamen length, and leaf). This is observed despite high and significant phenotypic correlations of flower length, pistil length, stamen length, and leaf size with corolla width, and points to some degree of independence in the genetic basis of the standing variation for these developmentally correlated traits. Further, it justifies our decision to forego MCIM methods in this experiment. QTLs in the wrong direction are, as expected, not pleiotropic with flower size (except for the two QTLs mentioned above), but in some cases do co-localize with each other (e.g. c4:LG13:e526). These QTLs are generally

additive, i.e. they are not QTLs like c4:LG4:e573 that had been hidden from selection in the outbred selection experiment.

2.3.1.3 Individual traits in putatively pleiotropic loci affect the trait in the same direction.

Every individual trait in every putatively pleiotropic locus affects the trait in the same direction. This argues for true pleiotropy rather than linkage explaining the co-localization of traits. Population size in the selection experiment was large, and selection was univariate (corolla width only) and short (only 6 generations). Further, the generation of F2 mapping populations was preceded by a generation of random mating to break down linkage disequilibrium. The conditions of the plant breeding that preceded the crosses, together with the consistency in direction of QTL effect, makes it unlikely that pleiotropic QTLs identified in this experiment are an artifact of the linkage map.

2.3.1.4 Consistency in individual dominance effects in pleiotropic QTLs for morphology.

Further evidence that pleiotropic QTLs reflect true pleiotropy rather than linkage comes from the consistency of dominance effects for individual traits, as expected from theory (Keightley and Kacser 1988).

2.3.1.5 Variation in individual dominance effects in pleiotropic QTLs for flowering time.

Inconsistent dominance effects are indicated by a red box in Table 9. Remarkably, the majority of instances where there is variation in dominance among individual traits at pleiotropic loci involve "whole plant" QTLs with flowering time as the outlier. Given the short, water limited growing season and the correlation of fecundity with flower and plant size, differential dominance has implications for the maintenance of variation at these loci through antagonistic pleiotropy (see discussion).

2.3.1.6 Many degrees of freedom in the standing variation for phenotypically correlated traits.

QTL analysis suggests that different floral organs can evolve co-ordinately or separately. Further, individual genetic control of different parts of the flower, as evidenced by variable pleiotropy in floral QTLs (Table 9), indicates that there is significant variation within the Iron Mountain population for aspects of floral allometry, i.e. stigma-anther separation and corolla length/width ratio. Generally, it is expected that QTLs that affect just one aspect of the flower would impact the length width ratio or stigma anther separation more than QTLs that increase both length/width and both pistil/stamen length. We present some examples in Figure 12 in which there is clear co-localization in allometry QTLs with single trait QTLs.

Complete results from QTL mapping with allometry traits are not presented because mapping on composite traits easily results in false peaks. For instance, two

small corolla length and width QTLs that affected the trait in opposite directions, if in linkage, would result in a disproportionately large effect on the length/width ratio in that region of the genome. This QTL would purely be an artifact of the linkage map, since loci separated by cM of genetic distance are unlikely to be in linkage disequilibrium in the natural population. Since QTL effects sizes are expected to approximate an exponential distribution skewed to undetected small effect QTLs (Dilda and Mackay 2002), such false peaks are to be expected when mapping on ratios or differences of multiple traits.

Individual genetic control is also evident for leaf size uncoupled from flower size (see Table 9, c3), though the majority of leaf QTLs also affect floral traits. We note that this bias may be due to enrichment for floral QTLs in the selection experiment, rather than reflecting the true genetic architecture of standing variation for leaf size. In any case it is evident that there is variation for leaf and floral characteristics to evolve together, or separately (Figure 12). This lability is in contrast to mapping studies in Arabidopsis where QTLs for leaf and flower traits did not overlap (Juenger et al 2005), and the low amounts of genetic covariance between the leaf and flower reported in the literature in diverse plant species (reviewed in Ashman and Majetic 2006).

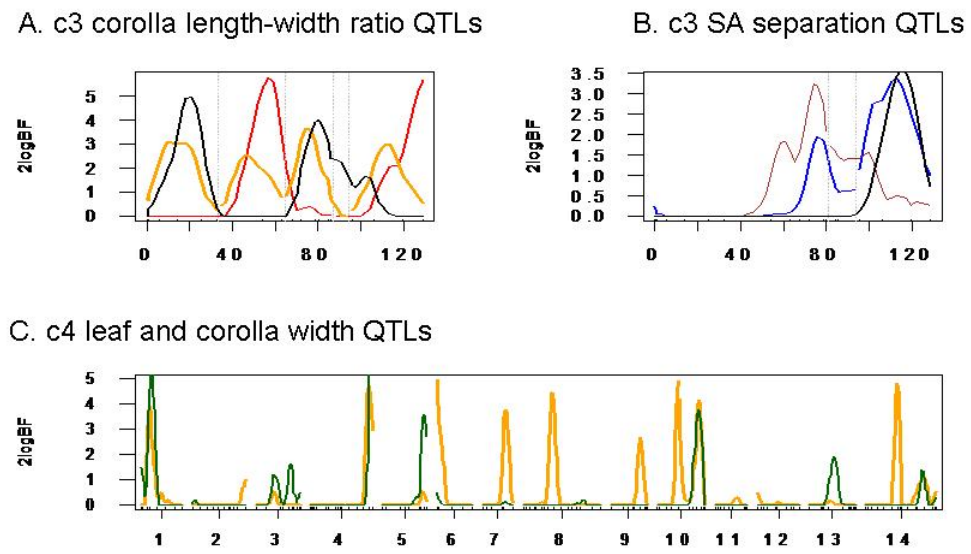

Figure 12: Many degrees of freedom in the standing genetic variation for phenotypically correlated traits. A. c3 LG8, orange line = corolla width, red line =corolla length, black line = length width ratio. Length width ratio QTLs coincide with regions of the genome that affect single traits i.e. corolla width. B. c3 LG8, purple line = stamen length, blue line = pistil length, black line = stigma anther separation. SA separation coincides with regions of the genome that affect single traits i.e. pistil length. Independent control of floral organs implies considerable variation for floral allometry. C.orange line = corolla width, green line = leaf width. We present all 14 linkage groups. Pleiotropic and independent QTLs are both observed, suggesting leaf and flower size can evolve coordinately or independently of each other. Y-axis in all figures: 2logBF, Bayes factor for the inclusion of a specific genomic region in the QTL model.

2.3.1.7 Most flower size QTLs are unique to cross.

We obtained the 50% highest probability density regions (HPD) for all corolla width QTLs and placed them on Figure 2 (the 3 linkage maps) in order to assess whether QTLs were mapped repeatedly in the different mapping populations (see dotted boxes in Table 9). Generally we were able to use shared markers in the HPD region to support co-localization of QTLs across the different mapping populations. The exception was the shared QTL on linkage group 7 which had large gaps in c3 linkage map.

Only 6 corolla width QTLs were mapped in 2 of 3 crosses (thus, about 1/3 of corolla width QTLs in Table 9) are shared. One of the 6 is the inversion. No QTL was mapped in all 3 crosses. In every case, the shared QTLs had different pleiotropic effects in the two crosses, for instance affecting only corolla width in one cross while affecting the whole flower in another cross. The variation in the mode of action of shared QTLs in independent crosses suggests there may be more than two alleles segregating at any given locus.

Should we expect to see more shared QTLs given that the parents of the mapping populations were extracted from an artificial selection experiment? While we can invoke epistasis to explain some of the unique QTLs (see section 2.3.4), we cannot directly address this possibility here. In any case we argue that the polygenic nature of loci, the existence of more than two alleles per locus, and the short duration of selection (6 generations) is adequate to account for the preponderance of unique QTLs. In Figure 13 we calculated expected allele frequencies in the selected populations after 6 generations of selection for a bi-allelic corolla width QTL of effect size a=0.1 from different starting frequencies (Griffing 1960), and from that calculated binomial probabilities for obtaining 0,1,2, or 3 F1 heterozygotes if the parents were randomly chosen from the selected populations and then crossed. For alleles at intermediate frequencies, F1 heterozygotes with QTL alleles in the wrong direction are unlikely after 6 generations (Figure 13a) and 1 or 2 F1 heterozygotes are more likely than 3 or 0 (Figure

13b, pink and green dots). Rare alleles dominating the selection response is unlikely given that almost all QTLs for corolla width were in the right direction.

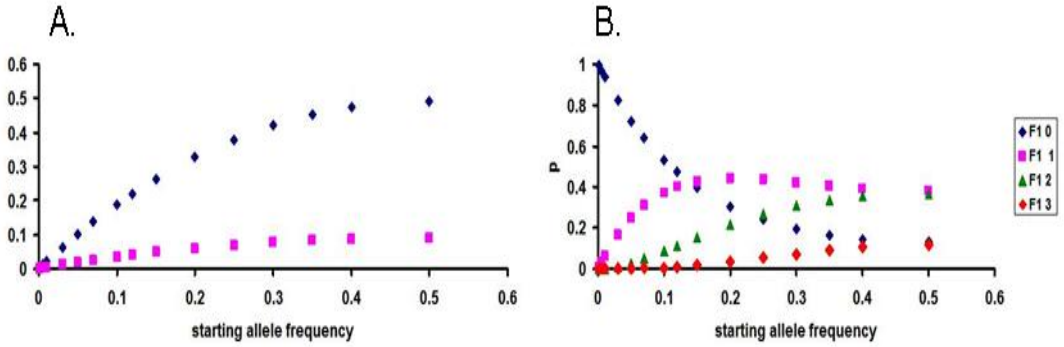

Figure 13: Expectations for heterozygosity in the F1s after 6 generations of selection given a QTL of effect size a=0.1. Expectations for a=0.1 (lower than the average of a=~0.25 for QTLs mapped in this experiment) are presented because the average effect of a QTL substitution estimated in a biallelic cross decreases in the context of a population (Valdor et al 2007). A. Probability of obtaining one heterozygote in the right direction (blue) and wrong direction (pink) after 6 generations of selection from different starting allele frequencies. B. Probability of having 0,1,2,3 heterozygous F1s in the right direction. Blue dots = 0 heterozygous F1s, pink dots = 1 heterozygous F1, green dots = 2 heterozygous F1s, and red dots = 3 heterozygous F1s.

2.3.2 QTLs for corolla width do not co-localize with inbreeding depression QTLs

We compare the location of deleterious QTLs for male and female fertility identified in chapter 1 with that of corolla width QTLs in Figure 14.

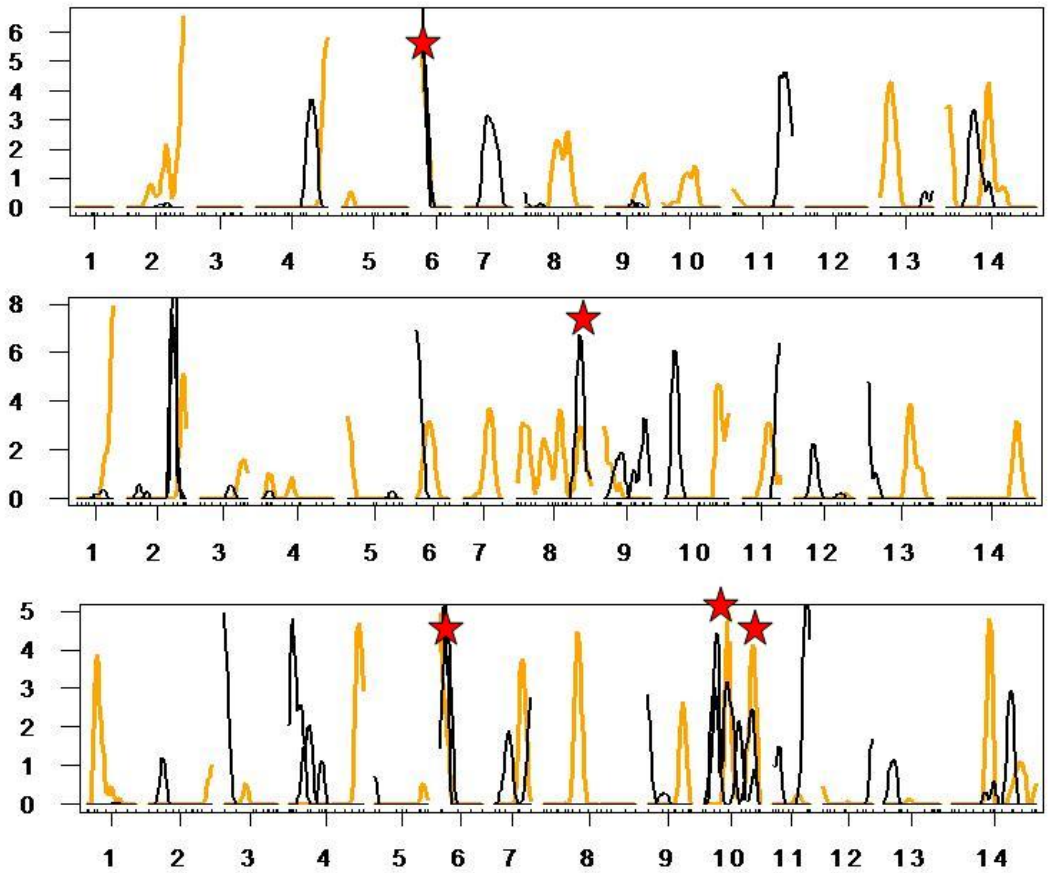

Figure 14: QTls affecting corolla width, seed set, and pollen inviability. Pollen number was excluded as it appears to have little influence on inbreeding depression for male fertility. c2, c3, and c4 mapping population results are stacked from top to bottom and we present all 14 linkage groups. Black lines = seed set or pollen viability QTLs. Orange lines = corolla width QTLs. Aside from the inversion (LG6) there are only 3 instances of co-localization between an inbreeding depression QTL and a corolla width QTL (indicated by a red star). Y-axis: 2logBF, Bayes factor for the inclusion of a specific genomic region in the QTL model.

There are only 3 instances of putative pleiotropy between inbreeding depression QTLs and corolla width QTLs aside from the inversion on LG6. While this conclusion is of course subject to power constraints, it is evident that the response to selection for

corolla width was not dominated by deleterious mutations for male and female fertility with pleiotropic effects on flower size.

2.3.3 Mode of action of QTLs for floral morphology, flowering time, and leaf width

We further present evidence that the genetic basis of morphological traits and flowering time is fundamentally different from inbreeding depression by examining their mode of action and effect size distributions (Figures 15 and 16).

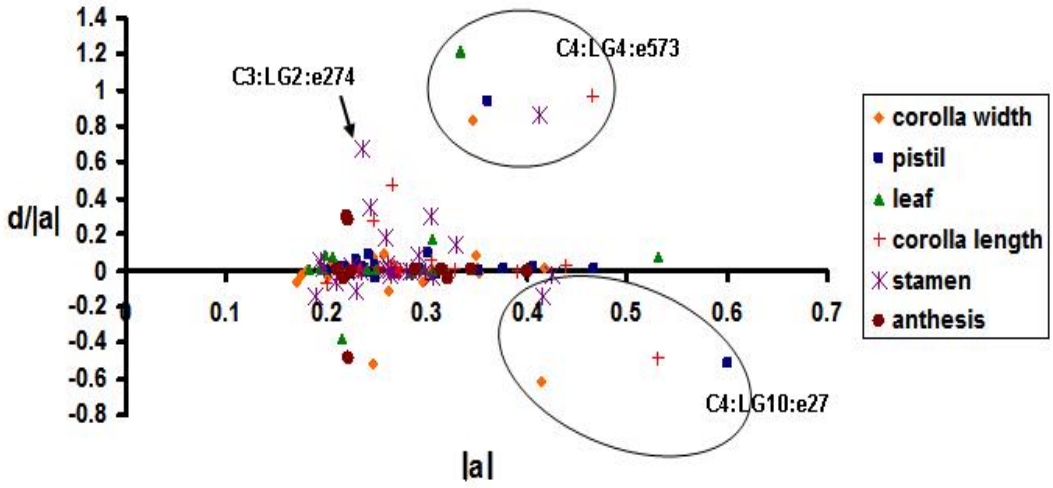

Figure 15: Mode of gene action for morphology and flowering time QTLs. Absolute additive effects on the x-axis, dominance ratio in the y axis. QTLs in circles map to the same putatively pleiotropic loci. C4:LG10:e27 also effects pollen viability (see Figure 14). We also indicate the major sterility/viability locus c3:LG2:e274 (see section 1.3.7), which affects stamen length.

Two "major" pleiotropic QTL (see Figure 16), indicated in circles, account for most of the outliers in dominance effects. QTLs for morphology and flowering time are clearly distributed around additivity ($d/|a| = 0$). There is no relationship with effect size

and dominance; larger QTLs are as likely to be additive as dominant for the increasing ($d/|a|>0$) or decreasing allele ($d/|a|<0$). This pattern is a clear contrast with the effect size and dominance relationship observed in QTLs for inbreeding depression in both viability and fertility, where there was a skew for recessive action of decreasing (deleterious) alleles as effect size increased.

Further, we note a difference in the effect size distribution (Figures 15 and 16). For inbreeding depression loci, effect size distribution was bi-modal. For morphology and flowering time loci, the effect size distribution is approximately exponential, concentrated around 0.2-0.25, with a continuous decrease in frequency as effect size increased.

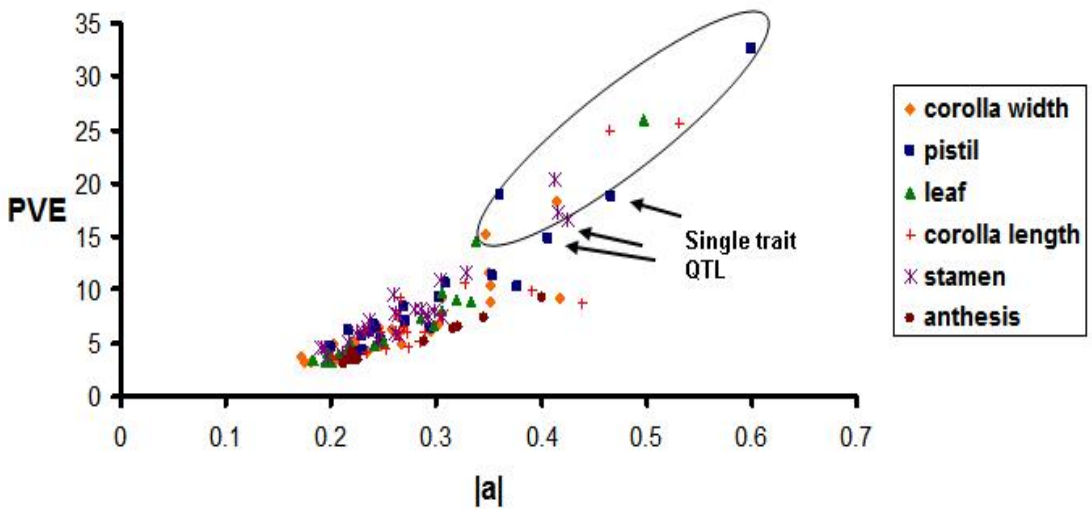

Figure 16: PVE (percent F2 variation explained) for morphology and flowering time QTLs. Two "major" QTLs, the same as highlighted within circles in Figure 15, account for most of the outlier loci (points within the circle, c4:LG4:e573 and c4:LG10:e27). The remaining outlier loci are all single trait QTL that affect pistil or stamen length (arrows).

While the bulk of standing variation for morphology and flowering time QTLs is accounted for by additive small-to-moderate effect loci, it is worth noting the two large effect, highly pleiotropic QTLs in the c4 mapping population that account for the outliers (Figure 15, 16). These two QTLs exhibit also near complete dominance in gene action, i.e the allele does not effect the trait in the heterozygote. This relationship between effect size, pleiotropy, and dominance has implications for the fitness effect of a mutation, i.e. it supports the assumption that mutations with large effects and/or extensive pleiotropy are more likely to overshoot optimum trait values and are thus deleterious (Orr 1998, 2000, Fisher 1930).

Finally, there are several large effect, independently acting, additive QTLs for pistil and stamen length (Figure 16). This implies that reduced (or expanded) stigma-anther separation can easily and quickly evolve from the standing variation on Iron Mountain, without constraint from correlated traits.

2.3.4 Epistasis contributes to standing variation for morphological traits

In Figure 17 we present evidence that epistasis contributes to standing variation for morphological traits. Further, we identify instances of epistasis which are also pleiotropic. All canonical forms of two locus epistasis was detected: additive-additive interactions (where the additive effect of a locus depends on the genotype at a second locus and vice versa), additive-dominant interactions (where the dominance at the first locus depends on the genotype at the second locus and the additive effects of the second locus depends on the genotype of the first locus) and dominance by dominance epistasis (where the dominance of the first locus depends on the genotype of the second locus and vice versa).

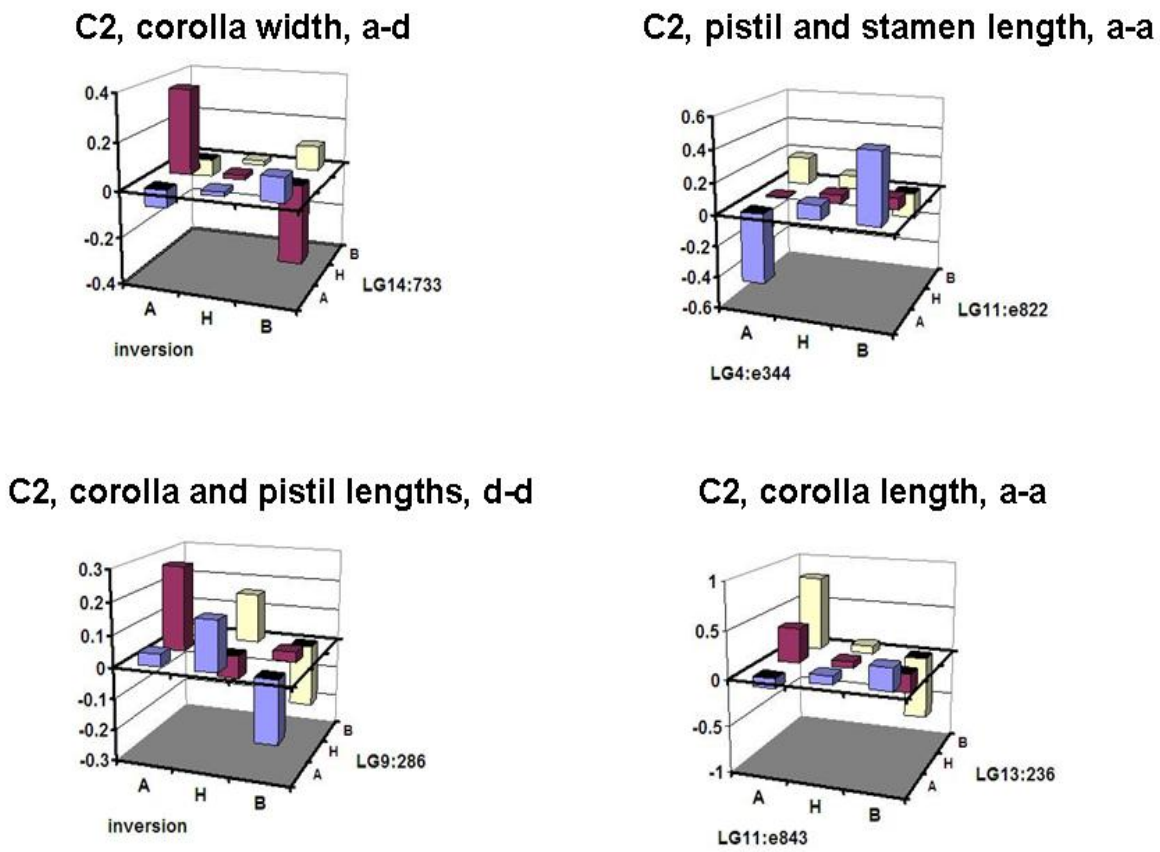

Figure 17: Epistatic interactions affecting floral morphology. Four epistatic interactions are presented, described above by cross, trait(s) affected, and the type of interaction. a-d: additive by dominant, d-d: dominance by dominance, a-a: additive by additive. Z axis is trait values in phenotypic standard deviations.

This experiment, with less than 400 individuals per F2 cross, was not designed to detect epistasis, suggesting that we identified only the largest and most significant interactions. PVE (percent F2 variation explained) for epistatic QTLs range from ~ 3 to 7 %, well within the range of effects observed for additively acting QTLs. It is noteworthy that in two of four epistatic interactions the inversion is involved as a partner,

suggesting that the inversion has potential to modify genetic covariances among traits in the Iron Mountain population.

2.3.5 Comparison with divergent QTLs

Finally, we present a comparison of the genetic architecture of standing variation for morphological traits with divergent QTLs mapped for the same traits in a recombinant inbred line (RIL) population between the perennial and annual ecotypes of guttatus (hereafter called the DUNxIM population).

The DunxIM population is not optimal for trait mapping for several reasons. There are only 172 lines, genotyping failure rate was high, and both cytoplasms segregate, effectively halving the sample size for QTL detection if the locus interacts with the cytoplasm. Only 3-5 QTLs were identified for each trait, which is surely a gross underestimate, and which renders effect size estimates suspect (Beavis 1994). Therefore we only assay a qualitative comparison of the pleiotropic relationships among different traits (Figure 18).

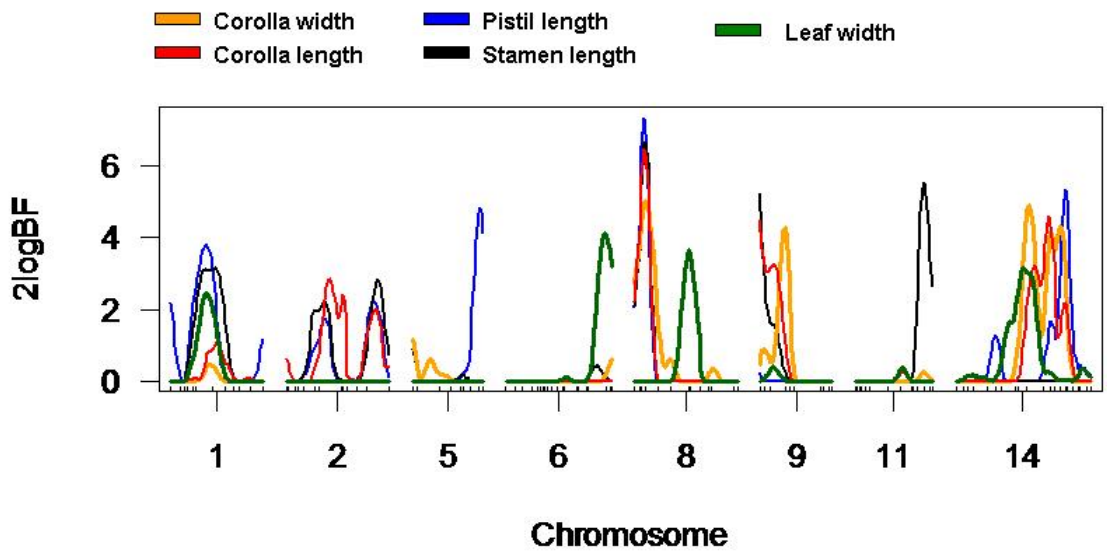

Figure 18: QTLs for floral and leaf morphology divergence between the perennial and annual ecotypes of guttatus. All QTLs were in the right direction, i.e. the bigger perennial parent carried the increasing allele.

We observed lability in genetic control of correlated traits in the standing variation, and the same is observed in the divergent QTLs. While most QTLs appear pleiotropic, there are exceptions for leaf width (LG6 and 8), pistil (LG5) and stamen length (LG11), where we identified single trait QTLs. Concordance in genetic architecture at two levels of divergence is consistent with trait diversification occuring through a process of conversion of the standing variation into interspecific fixed differences.

2.4 Discussion

2.4.1 Single biparental crosses are insufficient for describing the genetic architecture of standing variation.

From the c2 mapping population alone we would have concluded that floral traits are highly correlated, with variation for leaf size largely uncoupled from floral variation (Table 9). From the c3 population alone we would have concluded the opposite: different floral organs can vary independently from each other, and variation in leaf size is almost completely coupled to floral variation (Table 9). Without the c2 mapping population we would not have documented the role of the inversion in epistatic interactions affecting floral traits, with implications for the modification of genetic covariances between traits (Figure 17). The c4 population alone would have indicated that a good proportion of floral variation is accounted for by large effect loci that exhibit complete dominance, perhaps maintained by mutation selection balance (Figure 15).

Single biparental crosses result in a biased view of the genetic architecture of standing variation. This seems a truism, but one with implications for experimental design. Given the constraints of an experiment, is it desirable to do more crosses or bigger crosses? A broader view of the genetic architecture, or the power to describe a single genetic architecture really well? How the trade-off is resolved would depend on the specific goals of an experiment, but we note that the bias in a single biparental cross is worth considering even for crosses between evolutionarily divergent lines where

variation is assumed to be fixed. This is especially important if the parents are outcrossing species that harbor substantial amounts of standing variation. We further note the promise of association mapping approaches as well as multiparental crossing designs such as the Collaborative Cross (Yu et al 2006, Yu et al 2008, Macdonald and Long 2007) which may obviate the limitations of inference from biparental mapping populations in the future.

2.4.2 Maintenance of standing variation for flower size on in the Iron Mountain population

This genetic analysis, coupled with the results of Kelly and Willis 2001, indicates that flower size variation on Iron Mountain is controlled by alleles at intermediate frequency. The bulk of QTLs for morphological traits in the three mapping populations were almost all in the right direction, they are generally are additive, they are generally of small effect. As a useful contrast we also observed two "major" floral QTLs that exhibited almost complete dominance, and would not have contributed to the selection response (one of them was mapped in the wrong direction). The gene action of these "major" QTLs is consistent with rare deleterious mutations maintained by mutation and indeed one of the QTLs co-localizes with an inbreeding depression QTL. However QTLs with this mode of gene action were clearly the exception to the rule. The genetic dissection of variation for flower size (and correlated traits) strongly suggests that the standing variation is dominated by not-rare alleles at appreciable frequencies.

The varied pleiotropic consequences of flower size QTLs, coupled with what is known about environmental constraints in the growing season, easily lend itself to explicit balancing selection hypotheses. For example, overdominance could be induced by antagonistic pleiotropy in an allele that increases flower size (and seed set/pollen number) but also increases age at anthesis (detrimental, because later flowering exposes the developing fruit to drought). Conditions for maintenance of variation by antagonistic pleiotropy are less restrictive if there is reversal of dominance for fitness in different traits (Robertson 1967, Hedrick 1999, Rose 1982, Curtsinger et al 1994). While we cannot demonstrate this in a greenhouse experiment, we do observe differential dominance involving flowering time as the outlier in multiple pleiotropic loci. This is a remarkable repeated finding, and satisfies a necessary precondition for the maintenance of variation by antagonistic pleiotropy. We suggest a fruitful avenue for explicit tests of the hypothesis by evaluating QTL genotypes (and ultimately, alleles) of alternative homozygotes and heterozygotes in the field for their effects on the relevant traits and fitness components.

Another explicit hypothesis involves temporal variability in pollinator availability in the field. Contrasting directional selection for flower length/width ratio in the presence and absence of pollinators has been demonstrated on Iron Mountain in a manipulative phenotypic selection experiment (Fishman and Willis 2007). We observe that the pollinator distribution on Iron Mountain is patchy and may vary from year to

year. The QTL analysis indicates that there is abundant variation for evolution of floral allometry through the independent control of different floral components. Together, the heterogeneity in pollinators as a selective agent may result in the maintenance of variation at floral QTL. Explicit empirical evaluation of this hypothesis has implications for the evolution of selfing and the maintenance of mixed mating systems in the guttatus species complex, as well as the evolution of pollination syndromes (Fishman and Willis 2002, Galliot et al 2006, Stuurman et al 2004).

2.4.3 Relevance of standing variation for adaptation

Clearly, the genetic architecture of traits exhibiting inbreeding depression (chapter one) contrasts with that of morphological traits, suggesting that the variation for those two classes of traits are fundamentally different subsets (although examples like the inversion indicates some degree of overlap). This suggests that the standing variation is entirely relevant for long term selection and diversification of those traits, traditionally an open question for outcrossing species that exhibit considerable inbreeding load (Willis 1996).

Comparison of the genetic architecture of standing variation for floral morphology with that between divergent ecotypes and species may contribute to our understanding of the role of standing variation in adaptation and diversification. Previous studies on floral trait divergence in the *Mimulus guttatus* species complex have focused on *M. guttatus* and *M. nasutus,* which is thought to be derived from a guttatus-

like outcrossing ancestor (Fishman and Willis 2001, Fishman et al 2002). *M. guttatus* has typical floral characteristics for a bee-pollinated outcrosser, including a showy corolla with a broad throat and landing pads while *M nasutus* has very reduced corollas, including some cleistogamous buds, and self-pollinates before anthesis. QTLs segregating for perennial and annual ecotypes of *M. guttatus* have also been identified in an F2 cross (Hall and Willis 2005) and in RILs (section 2.3.5). Dune *guttatus* are large flowered perennials adapted to coastal sand dunes and differ from the Iron Mountain annuals in a suite of morphological and life history traits.

Both studies indicate polygenic distributions of QTLs for the traits measured similar to the standing variation. Significant genetic pleiotropy was observed for many QTLs in divergent crosses, but also variability in pleiotropic relationships (see section2.3.5). Interestingly, dominance estimates for QTLs distinguishing the selfer *nasutus* from the outcrosser *guttatus* had no bias towards either parent, which is perhaps consistent with gradual evolution of the selfer ecotype from the standing variation. In sum, while divergence in floral form could certainly have proceeded with input from new mutations, it is evident that fixed QTLs lack leading factors and have the same characteristics as segregating QTLs.

2.4.4 Many degrees of freedom for multivariate trait evolution

In addition to comparing standing genetic variation to existing QTL studies of trait divergence, we can also consider the "evolvability" of these traits. There is much

interest in the relative roles of developmental constraint versus natural selection in determining the extant and form of organismal diversity (Ashman and Majetic 2006, Kalisz and Kramer 2006, Brakefield 2006, Arnold 1992, Langlade et al 2005). In contrast, selection experiments often show that there is short term response even when the selection is conducted against the genetic covariance of traits, though there are exceptions for certain classes of traits (Frankino et al, 2007, Frankino et al 2005, Allen et al 2008, Holeski and Kelly 2005).

There are many degrees of freedom for multivariate evolution of floral form in the common monkeyflower. This is evident without invoking epistasis in the extensive yet variable pleiotropy of QTL alleles. While it has been suggested that the generally positive genetic correlations among traits predict the evolution of large outcrossing flowers (van Kleunan and Ritland 2004) genetic dissection indicates otherwise. There is variability for floral traits (as well as vegetative traits and development time) to evolve in myriad combinations, and change in the allele frequency at loci with pleiotropic effects can alter the G-matrix. The lability in genetic covariances indicated by our genetic analysis is concordant with the wide range of floral allometry and plant form observed in the *guttatus* species complex.

2.4.5 Epistasis and the evolution of the genetic variance and covariance

We document all forms of canonical digenic epistasis contributing to floral variation on Iron Mountain. The role of epistasis in trait evolution is hotly debated, with

mixed evidence when studied from a statistical versus a molecular framework. Here we only discuss epistasis insofar as to note that epistasis has the potential to "release" non-additive variation in the selection response especially in small populations (Carlborg et al 2004) and that epistasis has potential to modify of genetic covariances (Hansen 2006, Carter et al 2005). Given that studies indicate most genetic variance is additive (Hill et al 2008) the interesting outstanding question with regard to quantitative trait evolution is perhaps in the conditions and mechanism by which selection and linkage disequilibrium (as opposed to drift) can convert epistatic interactions into additive genetic effects (Gregerson et al 2006).

2.4.6 Conclusion

The genetic analysis standing variation for morphological traits suggests that variation for floral morphology (as well as leaf size and development time) is consistent with maintenance of a subset of the variation at intermediate frequencies. Flower size variation does not share the same genetic basis as inbreeding depression for fertility and viability, and as such is relevant for adaptation. Extensive and variable pleiotropy, as well as epistasis in the gene action of loci controlling standing variation has implications for the evolvability of traits. Concordance of the genetic architecture of standing variation with divergent QTL mapping studies within the same complex further supports the view that adaptation and speciation occurs by a process of conversion of the standing variation.

Bibliography

Allen, C. E., P. Beldade, B. J. Zwaan, and P. M. Brakefield. 2008. Differences in the selection response of serially repeated color pattern characters: standing variation, development, and evolution. BMC Evolutionary Biology 8:94.

Arnold, S. J. 1992. Constraints on phenotypic evolution. The American Naturalist 140: 85-107.

Ashman, T-L., and C. J. Majetic. 2006. Genetic constraints on floral evolution: a review and evaluation of patterns. Heradity 96:343-352.

Banerjee S. B. Yandell. and N. Yi. 2008 Bayesian Quantitative mapping for multiple traits. Genetics 179:2275.

Barrett, R. D. H., and D. Schluter. 2007. Adaptation from standing genetic variation. TRENDS in Ecology and Evolution 23:38-44.

Barton, N. H. 1990. Pleiotropic models of quantitative trait variation. Genetics 124:773-782.

Barton N. ands M. Turelli. 1989. Evolutionary quantitative genetics: how little do we know? Annu. Rev. Gen. 23:337.

Barton, N. H. and P.D. Keightley. 2002. Understanding quantitative genetic variation. Nature Reviews Genetics 3:11-21.

Birchler, J. A., D. L. Auger, and N. C. Riddle. 2003. In search of the molecular basis of heterosis. The Plant Cell 15:2236-2239.

Brakefield, P. M. 2006. Evo-devo and constraints on selection. TRENDS in Ecology and Evolution 21:362-368.

Byers, D., and D.M. Waller. 1999. Do plant populations purge their genetic load? Effects of population size and mating history on inbreeding depression. Ann. Rev. Ecol. Syst. 30:479-513.

Carlborg, O. and C. S. Haley. 2004. Epistasis: too often neglected in complex trait studies?. Nature Review Genetics 5:618-625.

Carlborg, O., L. Jacobsson, P. Ahgren, P. Siegel, and L. Andersson. 2006. Epistasis and the release of genetic variation during long-term selection. Nature Genetics 38:418-420.

Carr, D. E., and M. R. Dudash. 2003. Recent approaches into the genetic basis of inbreeding depression in plants. Proceedings of the Royal Society Series B 358:1071-1084.

Carter, A. J. R., J. Hermisson, and T. F. Hansen. 2005. The role of epistatic gene interactions in the response to selection and the evolution of evolvability. Theoretical Population Biology 68:179-196.

Charlesworth. B., and D. Charlesworth. 1999. The genetic basis of inbreeding depression. Genetical Research 74:329-340.

Charlesworth, D., and B. Charlesworth. 1987. Inbreeding depression and its evolutionary consequences. Annual Review of Ecology and Systematics 18:237-268.

Charlesworth B. , T. Miyo, and H. Borthwick. 2007. Selection responses of means and inbreeding depression of female fecundity in Drosophila melanogaster suggest contributions from intermediate freq alleles to quantitative variation. Genetical Research 89:85.

Charlesworth, B. 1992. Evolutionary rates in partially self-fertilizing species. Am. Nat. 140:126–148.

Cheng, R., A. Saito, Y. Takano, and Y. Ukai. 1996. Estimation of the position and effect of a lethal factor locus on a molecular marker linkage map. Theoretical and Applied Genetics 93:494-502.

Colosimo, P. F., C. L. Peichel, K. Nereng, B. K. Blackman, M. D. Shapiro, D. Schluter, and D. M. Kingsley. 2004. The genetic architecture of parallel armor plate reduction in threespine sticklebacks. PLoS Biology 5:635-641.

Crnokrak and Roff. 1999. Inbreeding depression in the wild. Heredity 83:260.

Curtsinger J., P. Service, and T. Prout. 1994. Antagonistic pleiotropy, reversal of dominance, and genetic polymorphism. Am. Nat. 144:210.

Dilda, C. L., and T. F. C. Mackay. 2002. The genetic architecture of Drosophila sensory bristle number. Genetics 162:1655-1674.

Fenster C. and K. Ritland. 1994. Quantitative genetics of mating system divergence in the yellow monkeyflower species complex. Heredity 73:422.

Fishman, L., A. J. Kelly, E. Morgan, and J. H. Willis. 2001. A genetic map in the *Mimulus guttatus* species complex reveals transmission ration distortion due to heterospecific interactions. Genetics 159:1701-1716.

Fishman, L., and J. H. Willis. 2007. Pollen limitation and natural selection on floral characters in the yellow monkeyflower *Mimulus guttatus*. New Phytologist 177:802-810.

Fishman, L., A. Kelly, and J. H. Willis. 2002. Minor QTLs underlie floral traits associated with mating system divergence in *Mimulus*. Evolution 56:2138-2155.

Fishman, L., and J. H. Willis. 2005. A novel meiotic drive locus almost completely distorts segregation in Mimulus (Monkeyflower) hybrids. Genetics 169:355-373.

Fishman and Saunders. 2008. Centromere associated female meiotic drive entails male fitness cost in monkeyflowers. Science 322:1559-1662.

Fishman L. J. Aagaard, and J. Tuthill. Toward the evolutionary genomics of gametophytic divergence. Evolution 62:2958-2970.

Frankino, W. A., B. J. Zwaan, D. L. Stern, and P. M. Brakefield. 2007. Internal and external constraints in the evolution of morphological allometries in a butterfly. Evolution 61:2958-2970.

Franco-Garcia A., S. Wang, A. Melchinger, and Z. B. Zeng. 2008. Quantitative trait mapping and the genetic basis of heterosis in rice and maize. Genetics 180:1707.

Galliot C., M. Hoballah, C. Kuhlemeier, and J. Stuurmann. 2007. Genetics of flower size and nectar volume in Petunia pollination syndrome. Planta 225:203-212.

Garcia-Dorado, A. V. Avila, E. Sanchez-Molano, A. Manrique, and C. Lopez-Fanjul. 2007. The build up of mutation-selection-drift balance in laboratory *Drosophila* population. Evolution 61:653-665.

Gardner, M. P., K. Fowler, N. H. Barton, and L. Partridge. 2005. Genetic variation for total fitness in *Drosopila melanogaster*: complex yet replicable patterns. Genetics 169:1553-1571.

Gillespie, J. H., and M. Turelli. 1989. Genotype-environment interactions and the maintenance of polygenic variation. Genetics 121:129-138.

Gregerson J. W. ,et al. Functional epistasis on a common MHC haplotype associated with multiple sclerosis. Nature 443:574.

Hackett, C. A., and L. B. Broadfoot. 2003. Effects of genotyping errors, missing values and segregation distortion in molecular marker data on the construction of linkage maps. Heredity 90:33-38.

Haldane, J.B.S. 1932. The causes of evolution.

Hansen T. The evolution of genetic architecture. 2006 Annu. Rev. Ecol. Evol. Syst. 37:123.

Hall, M. C., and J. H. Willis. 2005. Transmission ratio distortion in intrasoecific hybrids of *Mimulus guttatus*: implications for genomic divergence. Genetics 170: 375-386.

Hedrick P. Genetic polymorphism in heterogeneous environments: the age of genomics. Anu. Rev. Ecol. Evol. Syst. 37:67.

Hedrick, P.W. 1986. Genetic polymorphism in heterogenous environments: a decade later. Ann. Rev. Ecol. Syst. 17:535-566.

Hedrick P.W. 1999. Antagonistic pleiotropy and genetic polymorphism: a perspective. Heredity 82: 126-133.

Hedrick, P.W., M.E. Ginevan, and E.P. Ewing. 1976. Genetic polymorphism in heterogenous environments. Ann. Rev. Ecol. Syst. 7:1-32.

Hermisson, J. and P. Pennings. Soft sweeps – molecular population genetics of adaptation from standing genetic variation. Genetics 169:2335-2352.

Hill, W. G., M. E. Goddard, and P. M. Visscher. 2008. Data and theory point to mainly additive genetic variance for complex traits. PLoS Genetics 2:1-10.

Hochholdinger, F., and N. Hoecker. 2007. Towards the molecular basis of heterosis. TRENDS in Plant Science 12:427-432.

Holeski, L and J. Kelly. 2006 Mating system and the evolution of quantitative traits. Evolution 60:711.

Houle, D. 1992. Comparing evolvability and variability of quantitative traits. Genetics 130:195.

Houle, D., B. Morikawa and M. Lynch. Comparing mutational viabilities. Genetics 143:1467.

Jansen, J., A. G. de Jong, J. W. van Ooijen. 2001. Constructing dense genetic linkage maps. Theoretical Application Genetics 102:1113-1122.

Jarne, D., and D. Charlesworth. 1993. The evolution of the selfing rate in functionally hermaphrodite plants and animals. Annual Review of Ecology and Systematics 24:441-466.

Jeunger, T., G. M. Perez-Perez, S. Bernal, and J. L. Micol. 2005. Quantitative trait loci mapping of floral and leaf morphology traits in *Arabidopsis thaliana*: evidence for modular genetic architecture. Evolution & Development 7:259-271.

Jiang, C., and Z.B. Zeng. 1995. Multiple trait analysis of genetic mapping for quatitative trait loci. Genetics 140: 1111-1127.

Johnson T. and N. Barton. 2005. Theoretical models of selection and mutation on quantitative traits. Phil. Trans. Royal Soc. B. 360:1411.

Kalize, S. and E. M. Kramer. 2008. Variation and constraint in plant evolution and development. Heredity 100:171-177.

Keightley, P. D., and H. Kacser. 1987. Dominance, pleiotropy and metabolic structure. Genetics 117: 319-329.

Kelly, J.K. and J. H. Willis. 2002. A manipulative experiment to estimate biparental inbreeding in monkeyflowers. Int. Jour. Plant. Sci. 163:575.

Kelly, J. K. 2007. Testing the rare-alleles model of quantitative variation by artificial selection. Genetica 132:187-198.

Kelly, J. K. 2005. Epistasis in monkeyflowers. Genetics 131:1917-1931.

Kelly, J. K., and H. S. Arathi. 2003. Inbreeding and the genetic variance of floral traits in Mimulus guttatus. Heredity 90:77-83.

Kelly, J. K., and J. H. Willis. 2001. Deleterious mutations and genetic variation for flower size in *Mimulus guttatus*. Evolution 55:937-942.

Kelly, J. K. 2003. Deleterious mutations and the genetic variance of male fitness components in Mimulus guttatus. Genetics 164:1071-108.

Kelly J.K., A. Rasch, and S. Kalizs. 2002. A method to estimate pollen viability from pollen size variation. AMJB. 89:1021.

Keightley, P. D., and W. G. Hill. 1990. Variation maintained in quantitative traits with mutation selection balance - pleiotropic side-effects on fitness traits. Proceedings Of the Royal Society Of London Series B-Biological Sciences 242:95-100.

Keightley P. and A. Eyre-Walker. 1999 Terumi Mukai and the riddle of deleterious mutation rates. Genetics 153:515.

Kroymann, J. and T. Mitchell-Olds. 2005. Epistasis and balanced polymorphism influencing complex trait variation. Nature 435:95-98.

Kusterer et al. 2007 Analysis of a triple test cross design with RILs reveals a significant role of epistasis in heterosis for biomass related traits in Arabidopsis. Genetics 175:2009.

Langlade, N. B., X. Feng, T. Dransfield, L. Copsey, A. I. Hanna, C. Thebaud, A. Bangham, A. Hudson, and E. Coen. 2005. Evolution through genetically controlled allometry space. PNAS 102: 10221-10226.

Levene, H. 1953. Genetic equilibrium when more than one ecological niche is available. American Naturalist 87:331-333

Lande, R. 1975. The maintenance of genetic variability by mutation in a polygenic character with linked loci. Genetic Researches on Population Ecology 26:221-23.

Lande R. and D. Schemske. 1985. The evolution of self fertilization and inbreeding depression in plants. Evolution 39:24.

Lewontin, R. C. 1974. The genetic basis of evolutionary change. Columbia University Press, New York, NY.

Li, Z-K., L.J. Luo, H. W. Mei, D. L. Wang, Q. Y. Shu, R. Tabien, D. B. Zhong, C. S. Ying, J. W. Stansel, G. S. Khush, and A. H. Peterson. 2001. Overdominant epistatic loci are the primary genetic basis of inbreeding depression and heterosis in rice. biomass and grain yield. Genetics 158:1737-1753.

Lowry D., M. Hall, and J. Willis. 2009. in prep.

Luo, L., Y-M. Zhang, and S. Xu. 2005. A quantitative genetics model for viability selection. Heredity 94:347-355.

Macdonald, S. J., and A. D. Long. 2007. Joint estimates of quantitative trait locus effect and frequency using synthetic recombinant populations of *Drosophila melanogaster*. Genetics 176: 1261-1281.

MacKay, T. F. C., R. F. Lyman, and F. Lawrence. 2005. Polygenic Mutation in *Drosophila melanogaster*: mapping spontaneous mutations affecting sensory bristle number. Genetics 170: 1723-1735.

Malmberg, R. L., and R. Mauricio. 2005. QTL-based evidence for the role of epistasis in evolution. Genetical Research 86:89-95.

Malmberg R.L. and R. Mauricio. 2005. Epistsis for fitness related quantitative traits in Arabidopsis grown in the field and in the greenhouse. Genetics 171:2013

McCune, A. R., R. C. Fuller, A. A. Aquilina, R. M. Dawley, J. M. Fadool, D. Houle, J. Travis, and A. S. Kondrashov. 2002. A low genomic number of recessive lethals in natural populations of bluefin killifish and zebrafish. Science 296:2398-2401.

Melchinger A. et al 2007. Genetic basis of heterosis for growth related traits in Arabidopsis reveals a significant role for epistasis. Genetics 177:1872.

Mitchell-Olds, T. 1995. Interval mapping of viability loci causing heterosis in *Arabidopsis*. Genetics 140:1105-1109.

Mitchell-Olds T., J. Willis, and D. Goldstein. 2007. What evolutionary processes influence genetic variation for phenotypic traits? Nature Rev Gen. 8:845-856.

Orr, A. and A. Betancourt. 2001. Haldane's sieve and adaptation from standing genetic variation. Genetics 157:875.

Phillip, P. C. 2008. Epistasis – the essential role of gene interactions in the structure and evolution of genetic systems. Nature Review Genetics 9:855-867.

Reif, J. C., B. Kusterer, H-P Piepho. R. C. Meyer, T. Altmann, C. C. Schon, and A. E. Melchinger. 2009. Unraveling epistasis with triple testcross progenies of near-isogenic lines. Genetics 181:247-257.

Remington, D. L., and D. M. O'Malley. 2000. Whole-genome characterization of embryonic stage inbreeding depression in a selfed loblolly pine family. Genetics 155:337.

Ritland C. and K. Ritland. 1994. Variation of sex allocation among eight taxa of the mimulus guttatus species complex. AMJB. 76:1731.

Robertson A. 1967. The nature of quantitative genetic variation. In Heritage from Mendel, ed. RA Brink, pp. 265-80. Madison: University of Wisconsin press

Rose, M. R. 1982. Antagonistic pleiotropy, dominance, and genetic variation. Heredity 48:63-78

Scoville A. Y.W. Lee, J.H. Willis, and J.K. Kelly. 2009 Chromosomal polymorphisms and the G-matrix of Mimulus guttatus. In review.

Stuber C. et al. 1992 Identification of genetic factors contributing to heterosis in a hybrid from two elite lines of maize using molecular markers. Genetics 132:823.

Sweigart A., K. Karoly., A. Jones, and J. Willis. 1999. The distribution of individual inbreeding coefficients and pairwise relatedness in a population of Mimulus guttatus. Heredity 83:625.

Sweigart A. , L. Fishman, and J. Willis. 2006. A simple genetic incompatibility causes hybrid male sterility in Mimulus. Genetics 172:2465.

Shaw, R. G., S-M. Chang. 2005. Gene action of new mutations in *Arabidopsis thaliana*. Genetics 172:1855-1865.

Springer, N. M., abd R. M. Stupar. 2007. Allelic variation and heterosis in maize: how to do two halves make more than a whole. Genome Research 17:264-275.

Stam, P. 1993. Construction of integrated genetic linkage maps by means of a new computer package: JoinMap. The Plant Journal 3:739-744.

Stuurman, J., M. E. Hoballah, L. Broger, J. Moore, C. Basten, and C. Kuhlemeier. 2004. Dissection of floral pollination syndromes in petunia. Genetics 168:1585-1599.

Tallmon, D. A., G. Luikart, and R. S. Waples. 2004. The alluring simplicity and complex reality of genetic rescue. TRENDS in Ecology and Evolution 19:489-496.

Valdar W. et al. 2007. Genome-wide genetic association of complex traits in heterogeneous stock mice. Nature Genetics 38:879-887.

Van Kleunen M. and K. Ritland. Predicting evolution of floral traits associated with mating system in a natural population. Journal of Evolutionary Biology 17:1389.

Vogl, C., and S. Xu. 2000. Multipoint mapping of viability and segregation distorting loci using molecular markers. Genetics 155:1439-1447.

Wang S., C. J. Basten, and Z.-B. Zeng (2007). Windows QTL Cartographer 2.5. Department of Statistics, North Carolina State University, Raleigh, NC.

Willis, J. H. 1996. Measures of phenotypic selection are biased by partial inbreeding. Evolution 50:1501-1511.

Willis, J. H. 1999. The role of genes of large effect on inbreeding depression in Mimulusguttatus. Evolution 53:1678-1691.

Willis, J. H. 1999. Inbreeding load, average dominance, and the mutation rate for mildly deleterious alleles in Mimulus guttatus. Genetics 153:1885-1898.

Willis J.H. 1999. The contribution of male sterility mutations to inbreeding depression in Mimulus guttatus. Heredity 83:337.

Wu, C. A., D. B. Lowry, A. M. Cooley, K. M. Wright, Y.W. Lee, and J. H. Willis. 2007. *Mimulus* is an emerging model system for the integration of ecological and genomic studies. Heredity:1-11.

Xiao, J., J. Li, L. Yuan, S. Tanksley. Dominance is the major basis of heterosis in rice as revealed by QTL analysis using molecular markers. Genetics 140:745.

Yandell et al. 2007. R/qtlbim. Bioinformatics 23:641

Yi N. et al. 2005 Bayesian model selection for genome wide epistatic quantitative trait loci analysis. Genetics 170:133.

Yi N. et al. 2007 An efficient Bayesian model selection approach for interacting QTL models with many effects. Genetics 176:1865.

Yu, J., J. B. Holland, M. D. McCullen, and E. S. Buckler. 2008. Genetic design and statistical power of nested association mapping in maize. Genetics 178:539-551.

Yu, J., G. Pressoir, W. H. Briggs, I. V. Bi, M. Yamasaki, J. F. Doebley, M. D. McMullen, B. S. Gaut, D. M. Nielsen, J. B. Holland, S. Kresovich, D. S. Buckler. 2006. A unified mixed-model method for association mapping that accounts for multiple levels of relatedness. Nature Genetics 38:203-208.

Zhang, X., J. Wang, and W. Hill. 2004. Influence of dominance, leptokurtosis, and pleiotropy of deleterious mutations on quantitative genetic variation at mutation selection balance. Genetics 166:597-610

Zhang, X. and W.G. Hill. 2005. Genetic variability under mutation selection balance. TREE 20:468-470

Zeng, Z.B. 1994 Precision mapping of quantitative trait loci. Genetics 136:1457-1468

Biography

Young Wha Lee

Born June 7, 1979

Seoul, South Korea

Education

Ph.D., Genetics and Genomics, 2009: Duke University

B.A., Biology, 2002: Vanderbilt University

Publications

Scoville, A., **Y.W. Lee**, J.H. Willis, and J. K. Kelly. (2009) The contribution of chromosomal polymorphisms to the G-matrix of *Mimulus guttatus*. *In review*

Wu, C.A., D.B. Lowry, A.M. Cooley, K.M. Wright, **Y.W. Lee**, and J.H. Willis (2008). *Mimulus* is an emerging model system for the integration of ecological and genomic studies. Heredity 100: 220-230.

Xu, X., C.T. Hotta, A.N. Dodd, J. Love, R. Sharrock, **Y.W. Lee**, Q. Xie, C.H. Johnson, and A.R. Webb. Distinct light and clock modulation of cytosolic free Ca^{2+} oscillations and rhythmic *CHLOROPHYLL A BINDING PROTEIN2* expression in Arabidopsis. (2007). Plant Cell 19:3474.

Awards and fellowships received

Biology one-semester fellowship
Institute for Genome Sciences and Policy studentship
James B. Duke Fellowship